

Simulation of Particle Mixing and Separation in Multi-Component Fluidized Bed Using Eulerian- Eulerian Method: A Review

Yong Zhang^{*, 1, 2}, Zhenzhen Ran¹, Baosheng Jin¹, Youwei Zhang², Chunlei Zhou²
,Farooq Sher³

¹Key Laboratory of Energy Thermal Conversion and Control of Ministry of Education,
School of Energy and Environment, Southeast University, Nanjing, 210096, China

²Jiangsu Frontier Electric Technology Co., Ltd, Nanjing, 211100, China

³School of Mechanical, Aerospace and Automotive Engineering, Faculty of
Engineering, Environmental and Computing, Coventry University, Coventry CV1 2JH,
UK

ABSTRACT: In practical engineering applications, the mixing and separation behavior of multi-component particles is of great importance to the fluidized bed operation. The development of many practical processes is inseparable from the knowledge of particle mixing and separation, such as material processing of ash-soluble coal gasification, multi-phase flow in boilers, and petrochemical catalytic processes. In recent years, due to the obvious advantages of the Eulerian–Eulerian model, many researchers at home and abroad have used it to study the mixing and separation behavior of particles. This paper reviews the use of Eulerian–Eulerian model to study the mixing and separation of multi-component particles in fluidized beds. The Eulerian–Eulerian model describes

*Corresponding author. Tel.: +86-25-83794744; Fax: +86-25-83795508.

E-mail address: zyong@seu.edu.cn (Y. Zhang), Farooq.Sher@coventry.ac.uk (F. Sher)

21 the gas-phase and each of the individual particles as continuums. The mechanism of
22 particle mixing and separation, the influence of different factors on the particle mixing
23 and separation including differences in particle size and density, the differences in
24 apparent air velocity, the differences in model factors are discussed. Finally, an outlook
25 for the use of Eulerian–Eulerian model to study the mixing and separation behavior of
26 three component particles and related research on the drag model between particles.

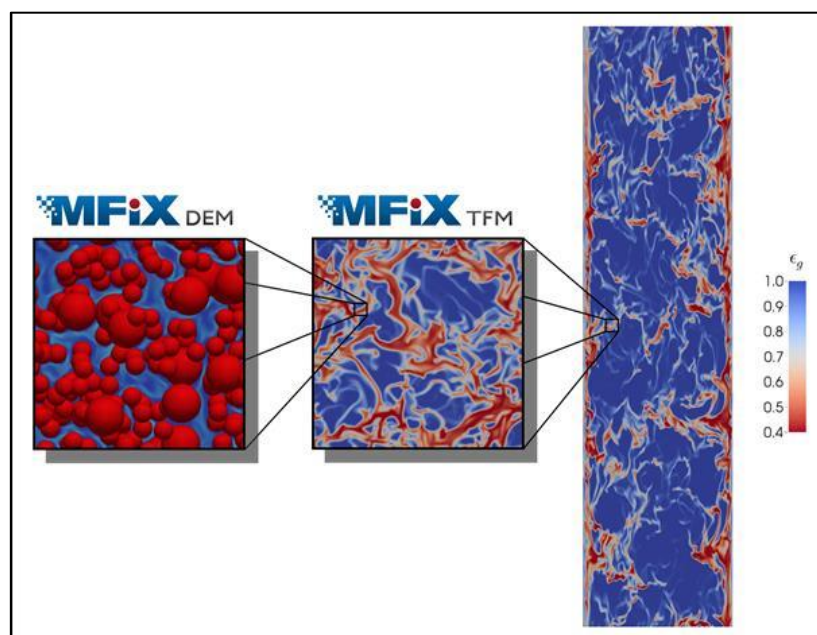
27 **KEYWORDS:** Multi-component Fluidized bed, Eulerian-Eulerian model, Particle
28 mixing and separation.

29 **1 INTRODUCTION**

30 Fluidized bed technology is widely used in energy, chemical, metallurgical,
31 pharmaceutical and other industrial fields. Because of high combustion efficiency, low
32 pollutant emission, strong fuel adaptability are consistent with the characteristic
33 advantages of energy development and it has received extensive attention and research.
34 However, it has internal dense gas and solid two-phase flow, high randomness and
35 variety. Therefore, it is difficult to study the numerical study with the complex factors
36 of coupling and solid-phase properties.

37 In an attempt to predict the internal dense gas and solid two-phase flow trends in gas-
38 fluidized beds, a wide variety of mathematical models have been used. There are two
39 calculation models of numerical simulation. One is Eulerian-Lagrangian model and the
40 other is Eulerian-Eulerian model. Figure 1 shows the difference between the Eulerian-

41 Lagrangian model and the Eulerian-Eulerian model. The Eulerian-Lagrangian model
42 uses two ways to research the fluid phase and particle phase: the fluid as a continuous
43 state and the particle as a discrete state. However, different phases are considered as
44 interpenetrating continua in Eulerian-Eulerian model. Because the Eulerian-Lagrangian
45 model is limited by the memory and speed of the computer, only a small number of
46 particles can be studied and the calculation process is simplified. And for fluidized bed,
47 flow-flow mixtures, etc., where the volume fraction of some second phases is not
48 negligible, the model has limitations. Therefore, when studying the mixing and
49 separation of a large number of particles in a fluidized bed, the Eulerian-Eulerian
50 method shows a significant operational advantage. Thus, using the Eulerian-Eulerian
51 model for the study of gas-solid two phase flow is the current development trend of
52 research.



53
54 **Figure 1:** The simulation method of Eulerian-Lagrangian model and Eulerian-Eulerian model.
55 (Tang, 2016).

56 The Eulerian-Eulerian model is a relatively mature model, and in recent years, with the
57 addition of some theoretical models, the Eulerian-Eulerian model has been improved.
58 In particular, the study of particle dynamics theory has greatly promoted the
59 development of the Eulerian-Eulerian model. Bagnold (Bagnold, 1954) began to
60 research on particle dynamics in 1954, and proposed the introduction of the original
61 equation of particle collision frequency. In the 1980s, Savage and Jeffrey (Savage and
62 Jeffrey, 2006) applied the theory of molecular motion to the theoretical study of the
63 smooth hard sphere model, and they assumed that the collision between particles was
64 purely elastic. Then, Jenkins and Savage (Jenkins and Savage, 2006) introduced the
65 particle-particle restitution coefficient and proposed energy consumption concept. In
66 order to better describe the movement of particles with different diameters and densities
67 in actual systems, in 1987, Jenkins and Mancini (Jenkins and Mancini, 1989) proposed
68 particle-based temperature definitions for multicomponent particle streams for two-
69 component particle phase systems. Subsequently, Alam et al. (Alam et al., 2002)
70 perfected the model and established particle models of different masses and sizes.
71 Based on non-Maxwellian velocity distributions and energy non-average assumptions,
72 Iddir and Arastoopour (Iddir and Arastoopour, 2005) applied particle dynamics theory
73 to multi-component (including size and density) particle systems. In their results, each
74 component particle is assumed to have an average velocity, turbulent kinetic energy and
75 particle pseudo temperature. Gidaspow et al. (Ding and Gidaspow, 2010) applied
76 particle kinetics theory to the particle continuous phase to save the computational

77 resources and to find the macroscopic particle motion state. Recently, a multiphase
78 model based on the kinetic theory of granular flow has been developed to study the
79 mixing behaviour of biomass and sand particles in a bubbling fluidized bed by Hameed
80 et al (Hameed et al., 2019). The accuracy of the model was verified by existing
81 experimental data, and the effects of various parameters such as surface gas velocity,
82 mixture composition and particle size were studied using the model.

83 The introduction of the drag model has further improved the Eulerian-Eulerian method.
84 The drag calculation model in the multi-particle system is based on the single-particle
85 drag model, and the particle volume fraction is introduced to correct the influence of
86 the surrounding particles, and then correlated with the particle Reynolds number and
87 volume fraction. There are two main methods: one is derived from the free
88 sedimentation process of the particles, such as the Richardson & Zaki model (Zaki and
89 Richardson, 1954); the other is derived from the fluidization process, such as Wen-Yu,
90 Ergun and Gidaspow models (Wen, 1966, Ergun, 1952, Ding and Gidaspow, 2010,
91 Gidaspow et al., 2004). Subsequently, some scholars made relevant corrections for the
92 problems of the basic model. Lu et al. (Lu and Gidaspow, 2003) gave a method to
93 modify the continuity of the Gidaspow model. Syamlal et al. (Syamlal and O'Brien,
94 1987) derived the drag force calculation formula based on the minimum Richardson-
95 Zaki velocity-porosity correlation. Vejahati et al. (Vejahati et al., 2009) proposed a new
96 correction method based on the particle balance characteristics and gas-solid velocity
97 characteristics at minimum fluidization velocity. The drag calculation model also

98 includes Gibilaro, Koch-Hill and Mckeen models, etc (Gibilaro et al., 1985, Koch and
99 Hill, 2001, Mckeen and Pugsley, 2003). Regarding the use of the drag model, the
100 researchers conducted a large number of related simulation calculations. Peng et al.
101 (Peng et al., 2009) studied the influence of classical Gidaspow model and improved the
102 Syamlal-O'Brien model on the gas-solid flow in a fluidized bed by comparing
103 theoretical calculation and experimental data. Esmaili et al. (Esmaili and Mahinpey,
104 2011a) used the Eulerian-Eulerian model for bubbling fluidized bed gas-solid two phase
105 flow for studying the Wen&Yu, Gibilaro, Gidaspow, Syamlal-O'Brien, Arastoopour, the
106 RUC, Di Felice, Hill Koch Ladd and a series of models for the movements of phase-to-
107 phase. Lin et al. (Lin et al., 2010) embedded the Koch-Hill and Mc Keen models into
108 Fluent through programming, and simulated the effects of the two and Gidaspow
109 models on the gas-solid two-phase flow in a two-dimensional bubble bed. The results
110 show that the Gidaspow model can realistically describe the shape of the bubble; the
111 Koch-Hill model predicts that the bed expansion is more obvious; the Mc Keen model
112 performs best in quantitative results. Li et al. (Li and Song, 2013) used Wen-Yu,
113 Gibilaro and Gidaspow drag models to simulate the gas-solid flow characteristics in a
114 bubbling fluidized bed. The results show that the Wen-Yu model produces large
115 prediction errors, while the Gibilaro model achieves better prediction results.

116 It is an important research direction to study the mixing and separation behavior of
117 multi-component particles. It has undergone the perfection of enlarging and theoretical
118 research from a single particle to multi-component particles and has done a lot of

119 theoretical research and experimental verification. The study on the mixing and
120 separation of multi-component particles using the Eulerian-Eulerian model is obviously
121 less than Eulerian-Lagrange model. However, the use of Eulerian-Eulerian model to
122 study the mixing and separation behavior of multi-component particles is a trend in
123 current research, and many scholars at home and abroad have studied the aspect. It is
124 the purpose of this work to provide an overview of the development of Eulerian-
125 Eulerian model was used to study the mixing and separation of multi-component
126 particles in the fluidized bed.

127 **2 MECHANISMS OF MIXING AND SEPARATION**

128 **2.1 Mechanisms of Bubble Dynamics**

129 The movement of bubbles has an important influence on the mixing of particles (Sitnai,
130 1981). The upward movement of the bubbles in the vertical direction, the confluence
131 of adjacent bubbles causes the lateral movement of the bubbles and the bursting of the
132 bubbles at the surface of the bed, which together contribute to the intense mixing of the
133 particles in the bed. The characteristic parameters such as the bubble size, speed and
134 the density of the bubbles play decisive roles in the pressure drop, density, porosity and
135 distribution of solid particles in the fluidized bed.

136 The bubble dynamics show that the movement of bubbles in the fluidized bed drives
137 the movement of the particles. Some scholars have studied the mechanism of the effect
138 of bubble motion on particle mixing and separation. Rowe and Nienow et al. (Nienow

139 et al., 1973b) and Lin et al. (Lin, 2010) found that the mixing and separation of two-
140 component particle systems in a gas-solid fluidized bed is caused by bubble motion.
141 Figure 2 shows a large number of bubbles are generated in the vicinity of the fluidized
142 bed distribution plate, and the deposition component entrained in the wake vortex
143 moves upward with the bubble, and when the bubble rises through the fluidized bed, a
144 local cavity is formed, and the hole will be filled by the upper particle. The whole
145 phenomenon shows that the particles are mixed at high gas velocity and separated at
146 lower gas velocity. The constant movement and exchange process causes the particles
147 to exhibit different distances of separation, resulting in separation. Scott Cooper et al.
148 (Cooper and Coronella, 2005a) researched the bubble behaviour, such as bubble growth,
149 bubble coalescence and bubble eruption, having a significant influence on the
150 mixing/segregation of binary particles. The simulation mainly studies the effect of mass
151 exchange mechanism between particle phase and bubble on particle mixing and
152 separation. Figure 3 shows the effect of bubble motion on particle separation. Figure 3
153 (a) indicates these velocity vectors changing over time, and Figure 3 (b) and (c) show
154 that point inspace beside the rising gas bubble. Studies have shown that the separation
155 effect between particles is due to the existence of smaller slip speeds. The apparent
156 particle slip velocity, though slight, its influence accumulates over the passage of both
157 time and additional bubbles.

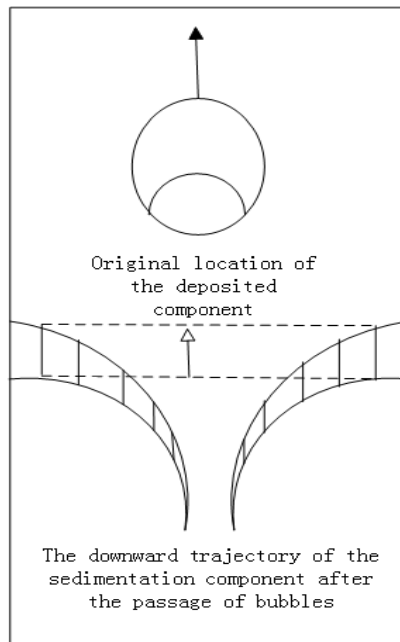
158 Some studies have shown that the rotation of the particles themselves or the rotation of
159 the bed structure itself will produce a large number of bubbles, which will have a certain

160 impact on the mixing and separation of the particles. Numerical analyses of effect of
161 particle rotation on gas and particles flow behavior were performed using two-fluid
162 flow model by Wang et al. (Wang et al., 2007) and Zhu et al. (Zhu et al., 2009).
163 Simulations show that bubbles are formed in the bed with particle rotation due to the
164 more energy dissipated by rotation. Due to the generation of bubbles, the variation of
165 particle concentration distribution in the bed is increased, which is more likely to
166 enhance the non-uniform structure of the bed. Liu et al. (Liu et al., 2016) used the
167 Eulerian-Eulerian model to simulate the flow characteristics of solid particles in an
168 internal swirling fluidized bed. The simulation results show that the bubbles in the
169 internal swirling fluidized bed are mainly generated on the high-speed wind side, and
170 the bubble generation is beneficial to the lateral and vertical diffusion effects of the
171 particles. The overall research results reveal that the structure of the bed is effective to
172 emerge a large amount of bubbles, which is conducive to the strong mixing of materials
173 in the bed.

174 The impact of bubble motion on particle mixing and separation in some specific cases
175 is also reported in related literature. Norway's mark Taylor university college B.M.
176 Halvorsen and B. Arvoh (Halvorsen and Arvoh, 2009) studied the fluidized bed with
177 different particle size minimum fluidizing gas velocity, bubble motion behavior and
178 pressure drop. By comparing the numerical simulation of bubble behavior with the
179 experimental results, it is found that the phenomena of bubble formation, pressure drop
180 and particle separation are basically the same. The document provides an effective way

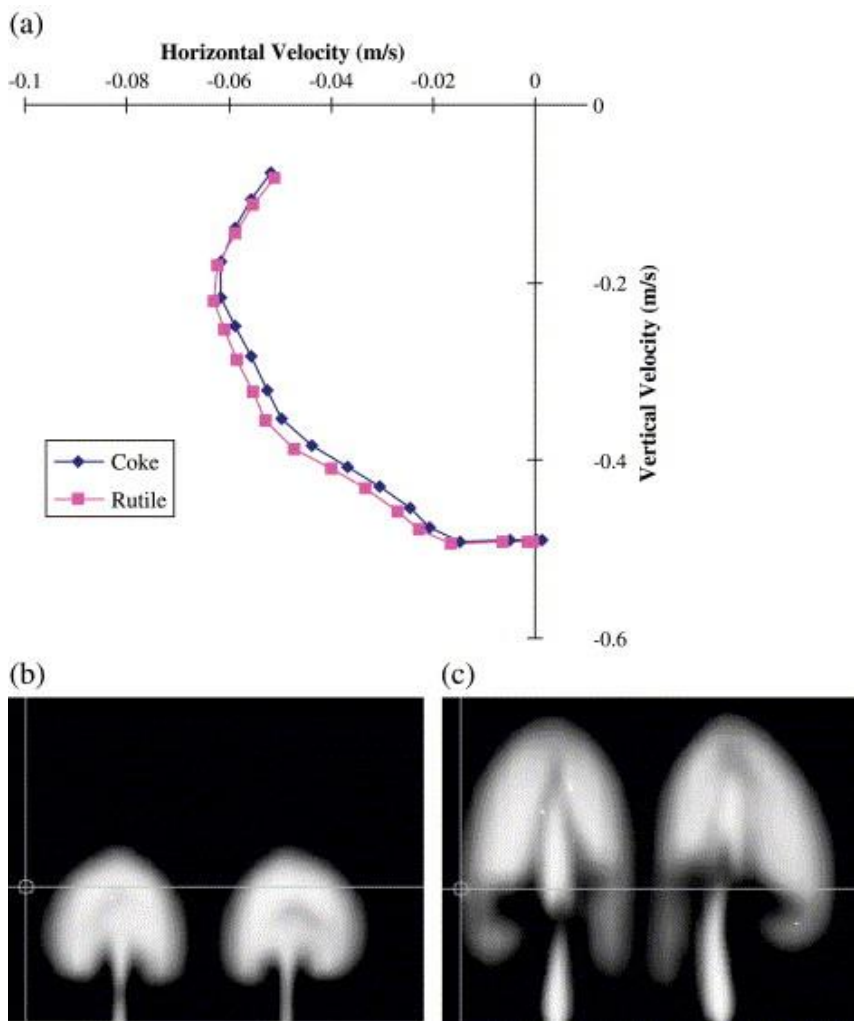
181 to study the motion behavior of bubbles in a fluidized bed in combination with
182 numerical simulation techniques. He (2012) used numerical simulation to study the
183 dynamic process of bubbles in aggravated fluidized bed. Exploring the effects of bubble
184 dynamics on the separation behavior in fluidized bed and the separation effect of
185 Geldart B particles. Computational Fluid Dynamics (CFD) simulations have been
186 carried out to examine the hydrodynamics of a mixture of biomass and biochar particles
187 in a bubbling fluidized bed by Sharma et al. (Sharma et al., 2014b). Figure 4
188 qualitatively shows the fluidization behavior of pinewood particles in the biochar bed
189 following by the bubbles motion at different superficial gas velocities ($u=0.45\text{m/s}$,
190 0.68 m/s , 1.14 m/s , 1.59 m/s). The results show that the bubbles starts forming only
191 at the minimum fluidization velocity, and this vigorous movement of particles with
192 bubbles favours the mixing of the solid phases of different densities and sizes along the
193 bed height. Because the segregation of binary particle mixtures is promoted by solids
194 movement around rising bubbles, the segregation mechanism can be identified by
195 tracking the velocity vectors of both solid phases near a passing bubble. And Cardoso
196 et al. (Cardoso et al., 2018) studied the effect of bubble dynamics on the mixing effect
197 of biomass particles. The research shows that biomass and sand particles movement
198 within the fluidized bed is promoted by gas bubbles flow along the bed height. And the
199 difference in frequency of bubbles formation and bubbles size leading to variation in
200 axial and lateral movements of solid phases in the bed. Wang et al. (Wang et al., 2015)
201 used a three-dimensional numerical study of the mixing and segregation of binary

202 particle mixtures in a two-jet spout fluidized bed based on an Eulerian-Eulerian model.
203 It is found that the segregation mechanism of binary particle mixtures can be identified
204 by tracking the velocity vectors of both solid phases near a passing bubble. Lim et al.
205 (Lim and Lim, 2019) found that the formation of bubbles generated more vigorous
206 motions within the fluidized bed and higher particle velocities, especially at the bed
207 surface where bubbles burst. Bubble formation generally promoted mixing and reduced
208 segregation between flotsam and jetsam in such pulsating fluidized bed systems. Lim
209 et al. (Lim and Lim, 2019) investigated the mixing and segregation behaviors of a
210 binary mixture in a pulsating fluidized bed using Eulerian-Eulerian model. The research
211 found that an increase in mean velocity increases the formation of bubbles and
212 promoted mixing of the flotsam and jetsam in the fluidized bed. The formation of
213 bubbles generated more vigorous motions within the fluidized bed and higher particle
214 velocities especially at the bed surface where bubbles burst. Bubble formation generally
215 promoted mixing and reduced segregation between flotsam and jetsam in such
216 pulsating fluidized bed systems



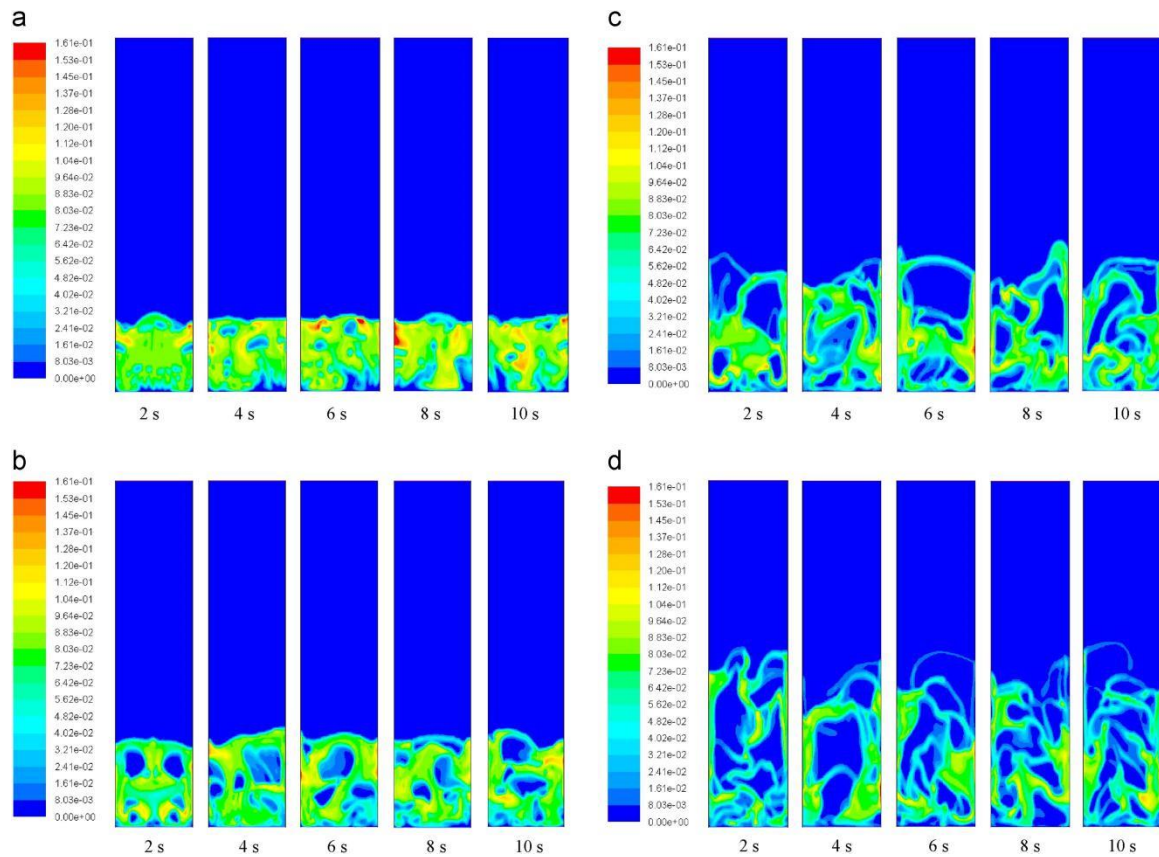
217

218 **Figure 2:** Schematic diagram of particle mixing and separation mechanism. (Nienow et al.,
 219 1973a).



220

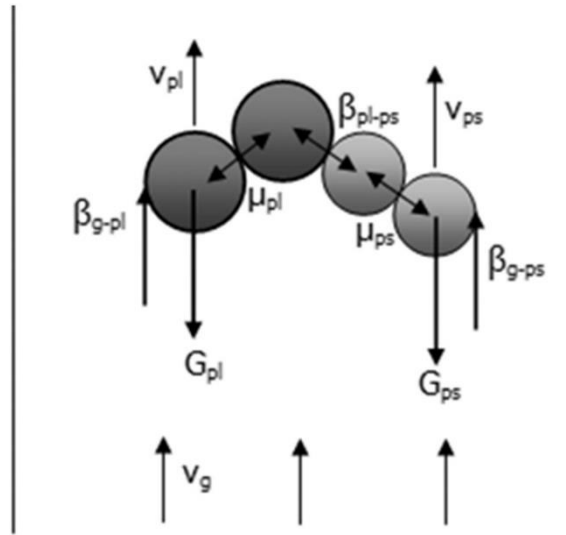
221 **Figure 3:** Illustration of segregation mechanism due to bubbling through a comparison of the
 222 velocity vectors for rutile and coke at fixed point $(x, y)=(0.006 \text{ m}, 0.050 \text{ m})$. (a) Each point is the
 223 endpoint of a velocity vector beginning at the origin. (b) Location of bubble relative to the fixed
 224 point at $t=0.20 \text{ s}$. (c) Location of bubble relative to the fixed point at $t=0.36 \text{ s}$. (Cooper and Coronella,
 225 2005a).



226
 227 **Figure 4:** Volume fraction profile of pinewood as a function of time at different superficial gas
 228 velocities. (a) $u=0.45 \text{ m/s}$ ($u/umf=1$); (b) $u=0.68 \text{ m/s}$ ($u/umf=1.5$); (c) $u=1.14 \text{ m/s}$ ($u/umf=2.5$); and
 229 (d) $u=1.59 \text{ m/s}$ ($u/umf=3.5$). (Sharma et al., 2014b).

230 2.2 The Drag Force Model Between Gas-Solid and Particle-Particle

231 In a gas-solid-solid system as illustrated in Figure 5, moving particles are subject to
 232 various forces including accelerating forces, gravity, solid-solid stresses, and inner
 233 stress in a solid phase. The accelerating force, include drag force, lift force and virtual
 234 mass force etc. And the drag force between gas-solid and particle-particle plays an
 235 important role in the mixing and separation of particles.



236

237

Figure 5: Forces and stresses in a binary particle system. (Du et al., 2016).

238

2.2.1 The Drag Force Model between Gas-Solid

239

There are three traditional drag models describing the interaction between the gas and

240

solid: one is the empirical or semi-empirical model based on the experimental data,

241

such as the Syamlal-O'Brien model (Gera et al., 1998) and the Gidaspow model (Yuan

242

and Gidaspow, 1990) . And the common feature of the model is the basis of the single

243

particle drag model, introducing the particle volume fraction function to describe the

244

effect of surrounding particles. The second is a model derived from a purely

245

mathematical method based on the theory of gas-solid interaction, such as the model of

246

Zhang et al. (Zhang and Reese, 2003) and the Koch-Hill model (And and Hill, 2001) .

247

The third is the modified empirical or semi-empirical model. The modified models,

248

such as the modified Syamlal-O'Brien model (Zimmermann and Taghipour, 2005), the

249

MeKeen model (MCKEEN et al., 2003).

250

Some scholars have studied the effect of traditional gas-solid drag model on the

251 movement of particles in a fluidized bed. Azizi et al. (Azizi et al., 2010) simulated the
252 size, density and combined size/density segregations in a bubbling fluidized bed with
253 different gas–solid drag models and found that the Wen-Yu drag model was suitable for
254 the simulation of these segregations. Based on the two-fluid model, Lin et al. (Lin, 2010)
255 adopted a three gas-solid drag models based on different mechanisms: the Gidaspow
256 model, the KochHill model and the McKeen model, and studied the gas-solid two-phase
257 flow by observing the bubble behavior. The study found that the McKeen model is more
258 accurate in calculating the bubble diameter quantitatively and in predicting the rate of
259 bubble rise, suggesting that the model can better predict particle mixing and separation
260 phenomena. Modeling the dynamic behavior of gas-solid flow in a pilot scale coal
261 beneficiation fluidized bed (CBFB) model was performed by Wang et al. (Wang et al.,
262 2013), a transient two-dimensional simulation was done based on two gas-solid drag
263 models together with the kinetic theory of granular flows. It can be drawn conclusions
264 that the Syamlal drag model gives better results than the Gidaspow model, as more
265 realistic bubble number and size, particle velocity distributions and bed density
266 distributions can be obtained. Sharma et al. (Sharma et al., 2014a) found that the choice
267 of gas-solid drag models had a considerable impact on the hydrodynamics of the
268 biomass-biochar mixture. Gidaspow, Syamlal-O'Brien and Huilin-Gidsapow model
269 have been considered. The simulation results show that the Syamlal-O'Brien and
270 Gidaspow models have similar trends in the prediction of results. However, compared
271 with the Syamlal-O'Brien and Gidaspow models, the Huilin-Gidsapow model predicts

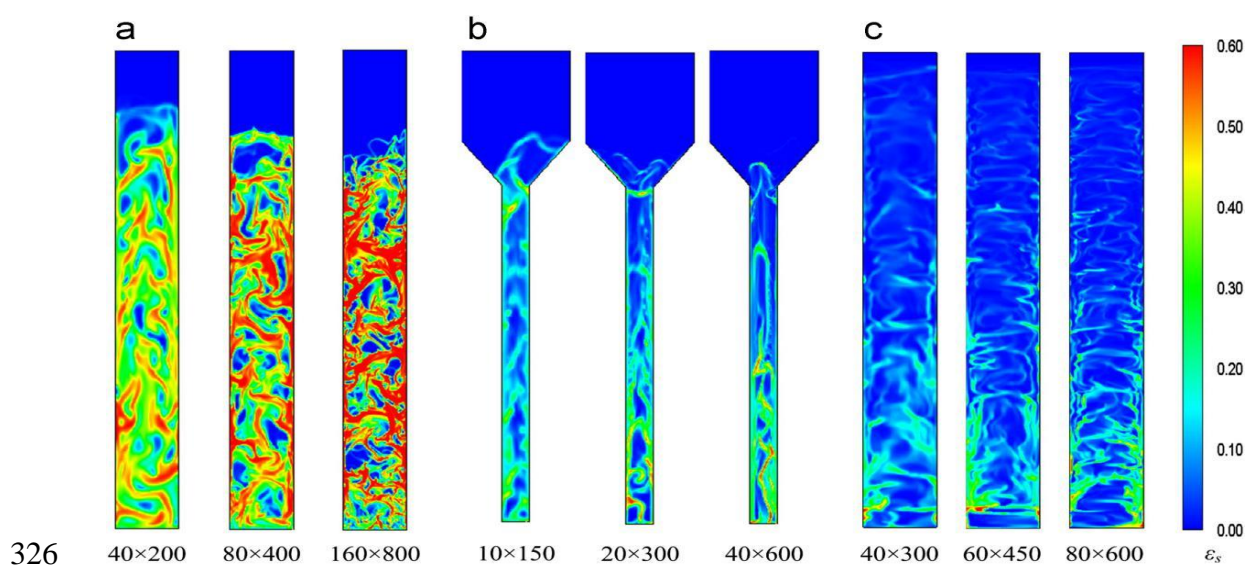
272 less separation between pine and biochar particles. Bakshi et al. (Bakshi et al., 2015)
273 modeled the hydrodynamics of dense-solid gas flows strongly affected by the Gidaspow
274 and Syamlal-O'Brien model. The results suggest that the Gidaspow model is more
275 applicable to homogeneous bubbling fluidization ($U/U_{mf} < 4$) while the Syamlal-
276 O'Brien model is only suitable for high velocities ($U/U_{mf} < 4$) associated with larger
277 bubbles and slugs.

278 However, for the traditional drag model, the gas-solid phase is generally based on the
279 research, so it is difficult to accurately predict the mixing and separation between
280 particles. The traditional gas-solid drag model is based on a gas-solid uniform structure,
281 which overestimates the drag between gas and solid and can not reflect well the non-
282 uniform flow structure in the fluidized bed. Therefore, in recent years, some scholars
283 have improved the model based on the traditional drag model. Using the concept of
284 minimum energy, Xiao et al. (Xiao et al., 2003) combined the traditional CFD method
285 with the macroscopic systematic analysis method to establish a new theoretical model
286 of gas-solid drag force for studying the particle agglomeration effect, which is
287 consistent with the experimental data, and find it universal. Compared with the existing
288 models, the new model not only has the same functional change relationship, but also
289 can reasonably describe the physical process of gas-solid two-phase interaction, and
290 predict the mixing and separation of particles accurately. Wang et al. (Yingce et al.,
291 2014) proposed a structure-based drag model. The new model takes into account the
292 influence of bubbles and mesoscale structures on the resistance, and more accurately

293 predicts the mixed motion state of the particles in the bed. Zheng et al. (Zheng et al.,
294 2015) obtained an improved drag model through a smooth function and coupled the
295 Eulerian-Eulerian model to numerically simulate a two-dimensional bubbling fluidized
296 bed. The study found that the improved drag model can better predict the agglomeration
297 between particles and more accurately show the internal circulation process of particles.
298 Wang et al. (Wang et al., 2018) extended the bubble-based drag model to binary hybrid
299 systems. The simulated results reveal that the bubble-based drag model captures a
300 relatively low bed expansion compared to the Gidaspow drag model and predicting the
301 mixing and separation of particles near the surface of the bed is more consistent with
302 measured data.

303 In recent years, the Yang Ning drag model based on the minimum energy multi-scale
304 (EMMS) (Yang et al., 2003) has been vigorously developed. Researchers have
305 combined the EMMS drag force with the complete two-fluid model to study the mixing
306 and separation effects of particles in a fluidized bed, and achieved good simulation
307 results. Hong, Kun et al. (Hong et al., 2013) proposed a new version of the bubble-
308 based EMMS model and verified it by comparison with experimental data. Figure 6
309 shows that uses the bubble-based EMMS drag model to study the gas-solid flow
310 conditions in the fluidized bed under three different conditions (bubbling fluidized bed,
311 turbulent fluidized bed, circulating fluidized bed) . In all, the bubble-based EMMS
312 drag predicts various heterogeneous structures in gas-solid fluidized beds, which agrees
313 qualitatively with experimental findings. Qi et al. (Haiying et al., 2014) studied the

314 EMMS model based on "theory of energy minimum multi-scale" (EMMS). The core of
 315 EMMS theory is to decompose the entire non-uniform flow into "particle dilute phase",
 316 "interaction phase" and "three uniform subsystems" (Li and Kwauk, 2003b). The study
 317 proposed different particle mass parameter models than all the existing drag models,
 318 which not only improved the model accuracy but also met the physical judgment. Chen
 319 et al. (Chen and Qi, 2014) used the particle cluster model to improve the EMMS drag
 320 model and numerically simulated the different working conditions. The flow
 321 characteristics of the fluidized bed of class A and B successfully predict the non-
 322 uniform distribution characteristics, local slip velocity, local non-uniformity and
 323 clogging state of the particles. The improved drag model more accurately predicts the
 324 mixing state of the particles in the bed and successfully captures the radial non-uniform
 325 distribution characteristics of the particles.



327 **Figure 6:** Snapshot of predicted solids concentration for (a): bubbling fluidized bed (Zhu et al.,
 328 2008), (b): turbulent fluidized bed (Venderbosch, 1998) and (c): circulating fluidized bed (Li and
 329 Kwauk, 2003a). (Hong et al., 2013).

330 **2.2.2 The Drag Force Model between Particle-Particle**

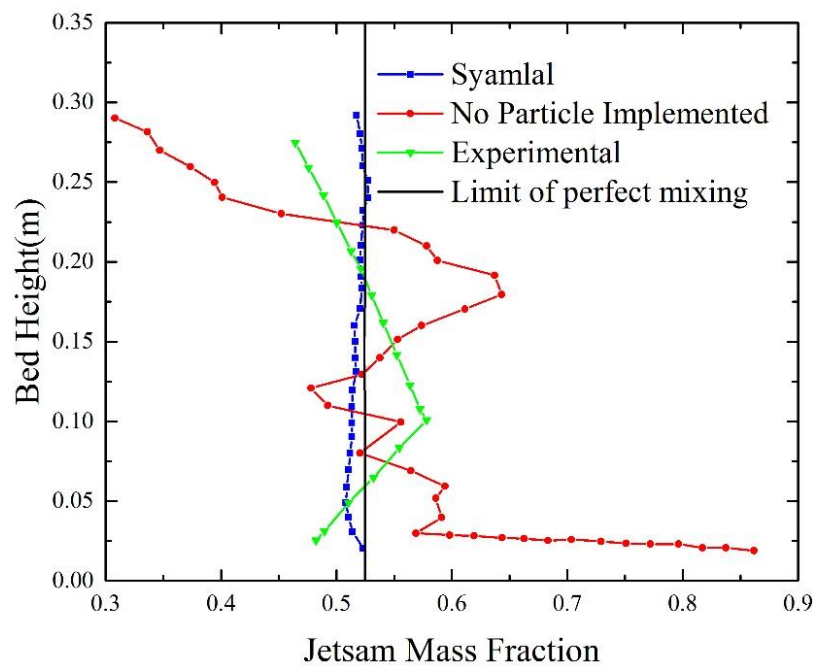
331 The difference between particle sizes and densities cause the difference in the
332 interaction between particles. The interaction between particles due to the generation
333 of the small slip velocity and the accumulation of small slip velocity between the
334 particles causes separation effect. The more common particle drag models are
335 Arastoopour, Gidaspow, Nakamura Syamlal, Bell, Syamlal and Dinesh Gera drag
336 models. Different drag forces between particles have their own using conditions and
337 scope; they can obtain relatively accurate results in their scope of applications.

338 Some studies have shown that considering the drag model between particles, it is
339 possible to better predict the separation effect between particles. Owoyemi et al.
340 (Owoyemi et al., 2010) studied the effect of interparticle turbulence on mixing and
341 separation by using the average of the particle phase instead of the usual solid phase
342 average. Four simulations have been carried out in Figure 7; three wherein different
343 constitutive equations for the particle-particle drag force are used, and a final one where
344 the force is entirely neglected. The three drag models Syamlal, Bell and Gidaspow
345 yielded similar results in terms of jetsam particle distribution within the bed, with an
346 almost perfect mixing and a good agreement with the experimental data. In the no
347 particle drag implemented case study, conversely, an overprediction of the jetsam
348 mobility is found with a resulting tendency of such phase to segregate toward the
349 bottom of the bed, which is in clear contrast with the experimental evidence. Li et al.

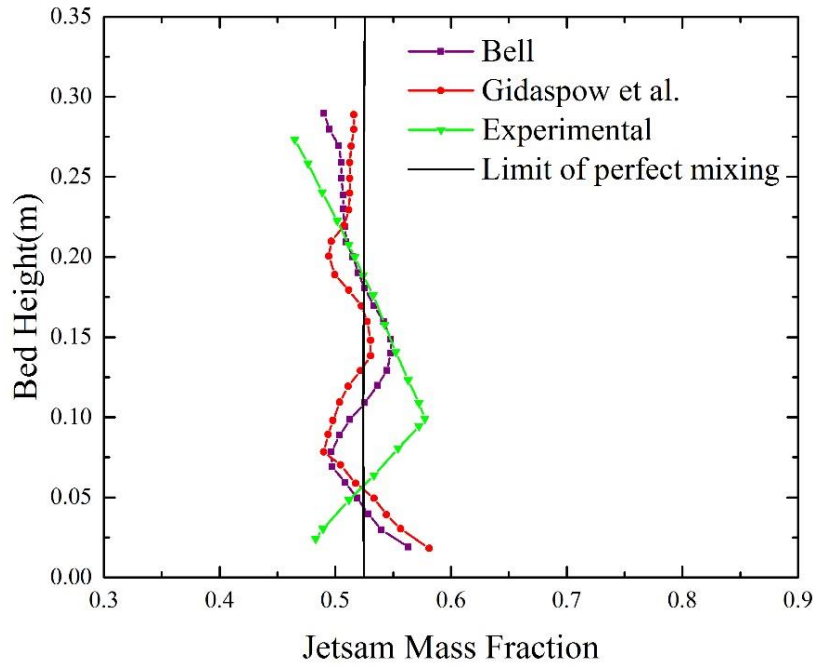
350 (Jun et al., 2013) based on the Eulerian-Eulerian model; a bubbling fluidized bed with
351 two different particle sizes in a bed was studied using numerical simulations. In addition,
352 the separation of large particles and small particles was investigated to the particle-
353 particle phase drag model. The results show that the gas can fully interact with the solid
354 particles considering the particle-particle phase drag model, indicating that the particle-
355 particle phase drag model in the numerical simulation can predict the gas-solid two-
356 phase flow in the bed more reasonably.

357 In order to better predict the interaction between particles, some scholars have improved
358 the drag model between particle-particle based on traditional models. Wang et al. (Wang
359 et al., 2012) based on the Eulerian-Eulerian model, a particle-particle drag model
360 considering particle slope coefficient of segregation was presented for simulation of the
361 bubbling fluidized bed with two different sizes particles and a uniform gas inlet. By
362 comparing the simulation results with Owoyemi's experimental results and numerical
363 simulation results, it is found that the model predicts and analyzes the characteristics of
364 particle mixing and separation in the bed more reasonably. Gan et al. (Gan et al., 2012)
365 showed that particle-particle drag played an important role in the separation and mixing
366 of multi-component particles. In the work, several drag law models (Non-particle-
367 particle drag force model (NPP-model), Syamlal model (SPP-model) and Bell model
368 (BPP-model)) are used to study their effects on particle segregation in a gas-solid
369 fluidized bed. Compared to Syamlal and Bell model, the non-particle-particle drag
370 model yields a significant particle separation in the axial direction, which is in good

371 agreement with the experimental values. However, the simulation results indicate the
 372 limited ability of both SPP-model and BPP-model to capture the particle segregation in
 373 the fluidized system. Zheng (Zheng et al., 2015) proposed an improved resistance
 374 model for the problem of particle resistance drop at low particle concentration
 375 conditions and used the Eulerian-Eulerian model to simulate the flow characteristics in
 376 a bubbling fluidized bed. The results show that the improved drag model predicts the
 377 radial particle concentration distribution better and predicts the local pressure drop of
 378 the bed better.



379



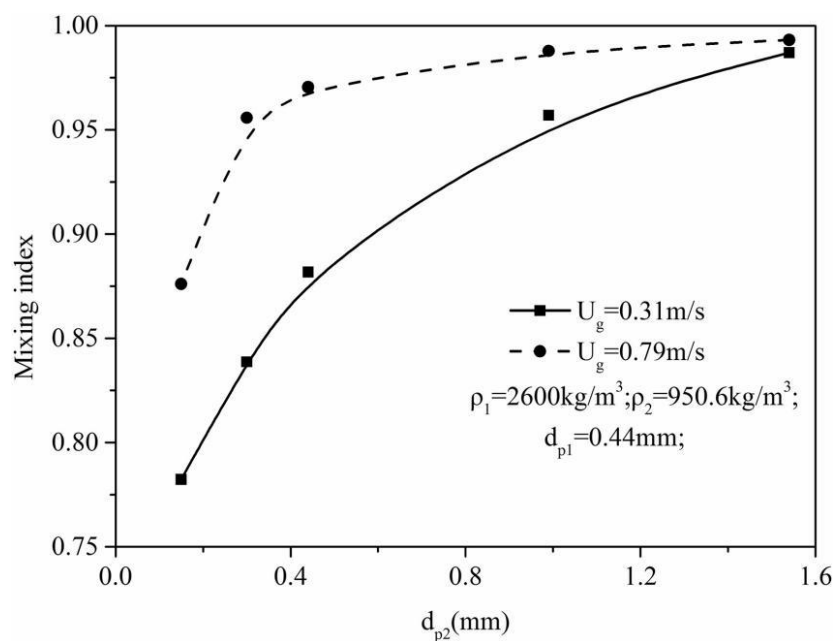
380

381 **Figure 7:** Comparison of computational and experimental segregation patterns (Syamlal, 1987, Bell,
 382 2000, Gidaspow et al., 1986). (Owoyemi et al., 2010).

383 **3 DIAMETER AND DENSITY AFFECTION MIXTURE** 384 **AND SEGREGATION**

385 The difference in particle size and density have a significant effect on the separation
 386 and mixing of particles. Solids mixing and segregation phenomena occur when a binary
 387 mixture is submitted to a fluidization process. Solids movement promoted by the air
 388 flux will induce a buoyancy effect, forcing the solid particles to arrange and find the
 389 equilibrium according to their size and density. Particles will then either segregate, if
 390 the size or density ratio is larger; or mix if the particles size or density ratio is lower.
 391 Depending on the composition of the particles, some researchers have defined the
 392 degree of mixing and the degree of separation (Murray, 1965, Bai et al., 1999, Rowe,
 393 1972, Shao and Lai, 1991, Peng et al., 2013). Following the Owoyemi et al. (Owoyemi

394 et al., 2010), the top 25% of the bed is chosen to calculate the top region. The variation
 395 of the mixing index with the jetsam particle size at different velocities is shown in
 396 Figure 8. It can be found that as the jetsam particle size decreases, the mixing index is
 397 reduced. When the operating velocity is reduced, the descending degree of the mixing
 398 index is enhanced. And it is mostly marked at low gas velocities especially when there
 399 is appreciable particle density difference. However, even a strongly segregating system,
 400 it can be fairly well mixed if the gas velocity is increased sufficiently (Rowe and Nienow,
 401 1976). Hence, a reasonable match of particle properties and operating velocity is a key
 402 to achieve the segregation of a binary mixture. (Cardoso et al., 2019)



403

404 **Figure 8:** Variation of mixing index with jetsam particle size at different velocities. (Owoyemi et
 405 al., 2010).

406 3.1 System of Two-Component Particles

407 When two-component particles by different size or density of the composition, which

408 one has a lower minimum fluidization velocity of the particle (flotsam) are first
409 fluidized, and another has a large minimum fluidization velocity of the particle (jetsam)
410 is still filling state. Therefore, the basic fluidization characteristics of two components
411 the system is more complex than the single is not necessary to promote mixing
412 component system. The fundamental reason for the separation or mixing of particles in
413 the fluidized bed is due to the rising movement of the bubbles (Sinclair, 1994,
414 Hoffmann et al., 1993) that we have explained before in the study of the mechanism. In
415 recent years, many scholars have done some researches on the influence of mixing and
416 separation on two-component particles density and size. The following will briefly
417 summarize the research results of domestic and foreign scholars.

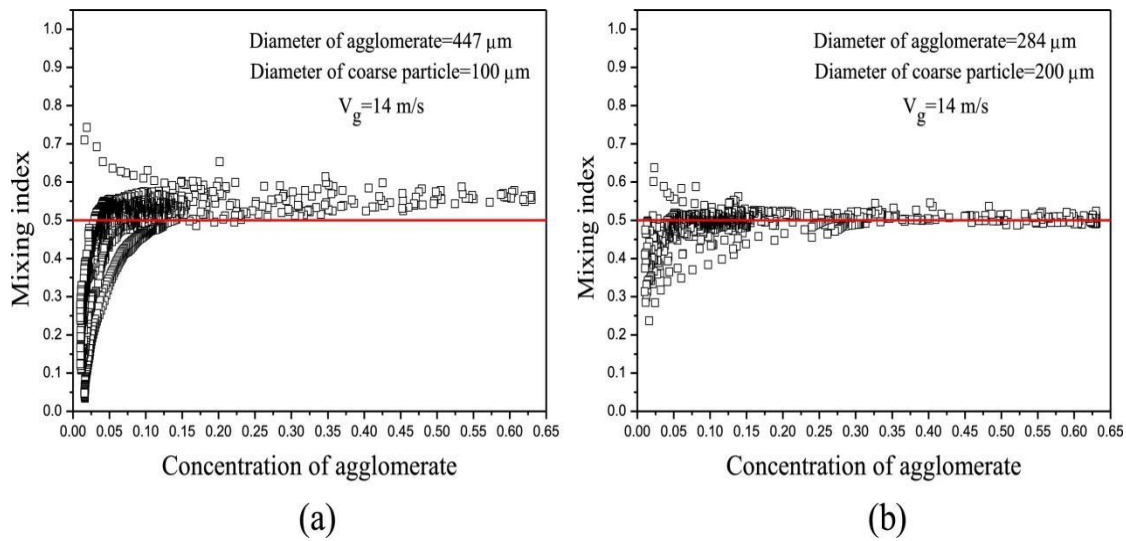
418 Some studies have shown that particle size differences in two-component systems have
419 a significant impact on particle mixing and separation systems. The fluidization
420 behavior of binary mixture differing in size in the gas bubbling fluidized bed is
421 experimentally and theoretically studied by Lu et al. (Lu et al., 2003b). The research
422 reveals that the fluidization behavior of a binary mixture differing in particle sizes with
423 the same density is strongly influenced by the variations of average particle diameter in
424 the bed. Reddy et al. (Reddy and Joshi, 2009) used the Eulerian-Eulerian model to
425 simulate the mixing and separation of two-component particles. The report found that
426 when there are certain particle size difference between particles, some segregation
427 occurs; when the difference in particle size is small, the two particles are completely
428 mixed in the flowing state. Mostafazadeh et al. (Mostafazadeh et al., 2013) and Zhong

429 et al. (Zhong et al., 2016) studied the distribution of particles in a two-component
430 system with different particle sizes at different superficial gas velocities. The research
431 demonstrates that in the initial state, a mixture of large and small particles uniformly
432 mixed at a certain height is accumulated in the bed. At the lower gas velocity, the two
433 kinds of particles are classified according to the difference in particle size. During the
434 large particle classification process, they are deposited on the bottom of the bed, while
435 the small particles are concentrated on the top of the bed.

436 In the multi-component fluidized bed system, the effect of the difference in particle
437 density on the motion behavior of the particles is also studied. Chao et al. (Zhongxi et
438 al., 2012) used a two-fluid model to study the segregation behavior of two types of
439 particles with approximately same particle diameters and different particle densities in
440 a dense binary gas fluidized bed. The simulation result shows that the jetsam and
441 flotsam are segregated apparently axially; generally, there are lighter flotsam in the top
442 of the bed and more heavy jetsam near the bottom. Zhang et al. (Zhang et al., 2004)
443 selected a representative non-equal density/diameter two-component system (resin and
444 sand) as the research object, and used the Eulerian-Eulerian model to simulate the
445 motion behavior of two-dimensional cold-mode jet bed particles. The study found that
446 the local circulations exist randomly in the global circulating flow in a two-component
447 particle system. Solid circulation pattern is divided into three regions : jetting region ,
448 bubble street and annular region, which results in strong mixing of particles. The effect
449 of biomass density and particle size on the mixing/segregation behavior of biomass-

450 biochar mixture was analyzed using the Eulerian-Eulerian model by Sharma et al.
451 (Sharma et al., 2014a). It is found that by changing the density of the biomass particles
452 while keeping the gas velocity constant, the mixing state of the two-component particles
453 can be greatly changed. Since the biomass component content is relatively small in the
454 whole, the change in the degree of biological plasmid does not change the overall
455 mixing and separation state of the system. The aggregation process and flow behavior
456 of ultrafine powders in a spouted bed were simulated and analyzed under varying
457 operating conditions with a two-fluid model coupled by Sun et al. (Sun et al., 2017).
458 Figure 9 shows the mixing behavior of ultrafine and coarse particles and illustrates the
459 agglomerate diameter as a function of fluidization time for two different conditions.
460 From the Figure 9, we can see that under the effects of inter-particle force, ultrafine
461 particles form agglomerates when collisions occur, and the agglomerate diameters
462 increase with fluidization time, and for the case with coarse particles, the agglomerate
463 diameter at a steady state is smaller than that without coarse particles because of the
464 cutting and isolation effects. The mixing behavior demonstrates that the coarse particles
465 may perform better when effectively mixed with bed materials. The results demonstrate
466 that the movement of the coarse particles weakens the strong inter-particle force
467 between ultrafine powders and breaks agglomerates into smaller ones, and effective
468 mixing will lead to improved coarse particle performance. Hassen et al. (Hassen et al.,
469 2018) used the Eulerian-Eulerian fluid model to simulate the cold flow of a gas-solid
470 mixture in a G-Volution circulating dual gasification reactor. The mixing and

471 segregation dynamics of a binary solid mixture of biomass ($\rho = 426 \text{ kg/m}^3$, $d = 0.856 \text{ mm}$)
 472 and sand ($\rho = 2650 \text{ kg/m}^3$, $d = 0.385 \text{ mm}$) with different size and density were considered.
 473 The result shows that a visible segregation of the biomass that rises above the sand
 474 particles is observed. This is due to the density which has the dominating effect and the
 475 denser component act as jetsam.



476 (a) (b)
 477 **Figure 9:** Agglomerate mixing index profile in the spout bed as a function of concentration: (a)
 478 100µm and (b) 200µm. (Sun et al., 2017).

479 3.2 System of Three-Component Particles

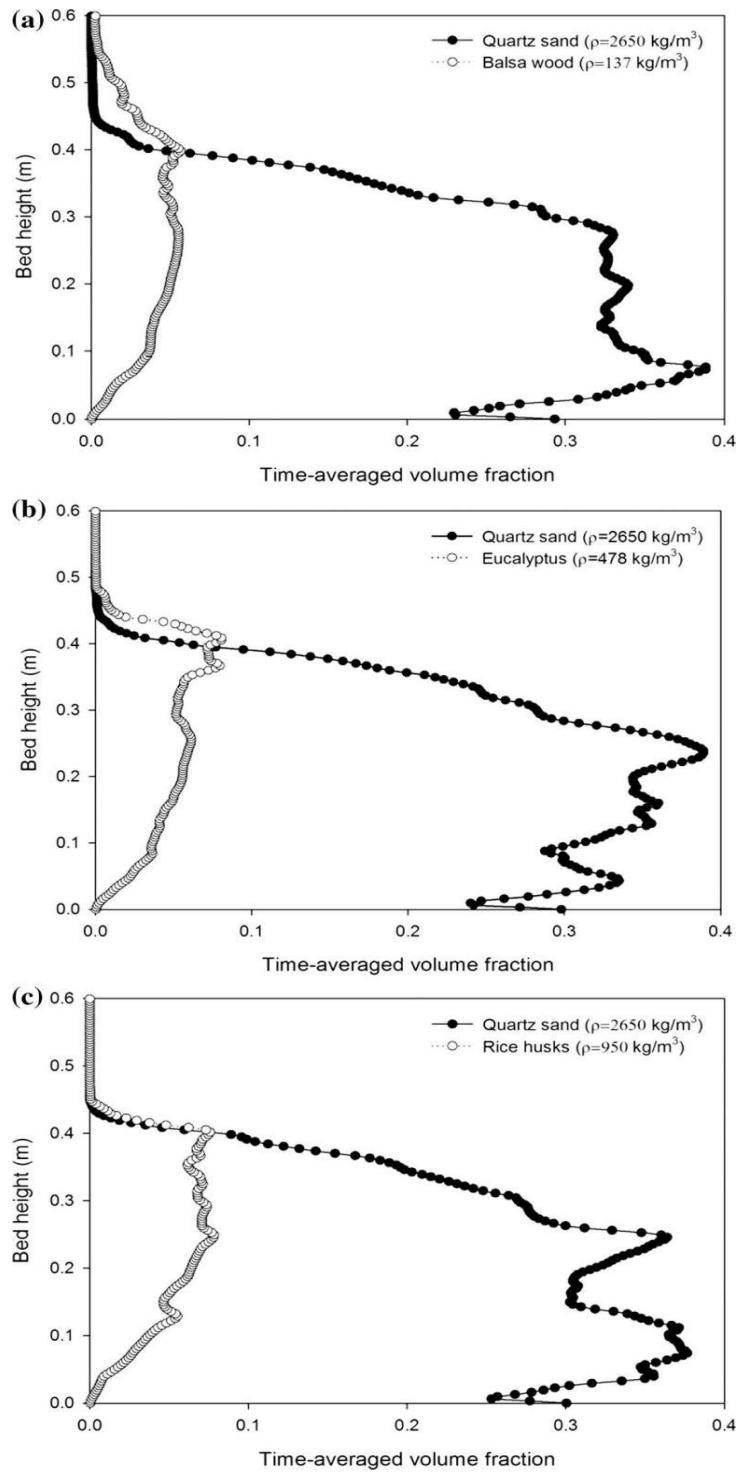
480 In actual industrial production, many materials are made up of two or more obviously
 481 different materials. The particle size and apparent density of different particles in a gas-
 482 solid fluidized bed have different effects on fluidization characteristics. There is a
 483 strong interaction between the gas in the fluidized bed and the particles and the mixing
 484 and separation mechanism of the three-component or even multi-component particle
 485 system particles is more complicated than the two-component particle system. In

486 practical engineering, most of the research objects are composed of three-component
487 or even multi-component particle systems. Therefore, it is more practical to study the
488 three-component or even multi-component particle system.

489 Some literature indicates that in a three-component particle system, the difference in
490 particle size leads to the separation effect between particles. Mathiesen studied
491 (Mathiesen et al., 2000) the flow behavior in a circulating fluidized bed by
492 approximating a realistic PSD as three discrete particle sizes. A realistic description of
493 the particle size distributions in gas/solids flow systems, the three solid phases have
494 diameters of 84, 120 and 156 μm , respectively. Through the simulation, the research
495 finds that the vertical segregation is observed for a wide PSD, and segregation for a
496 narrow PSD. Wang et al. (Wang et al., 2018) investigated the mixing and segregation
497 performance of binary mixture. Here, different biomass particle diameters (0.15mm,
498 0.3mm, 0.44mm, 0.99mm and 1.54mm) are chosen. The segregation behavior of the
499 second solid phase for different sizes can be observed at the operating velocity. As the
500 particle size decreases, the segregation phenomenon becomes significant owing to its
501 descending minimum fluidization velocity. Liu et al. (Liu et al., 2003) based on the
502 kinetic theory of dense gas molecules and particle dynamics, the interaction between
503 particle-particle in multi-component particles, the interaction between gas-particles are
504 considered. The study proposed a multi-component particle, non-isothermal particle,
505 gas-solid two-phase flow model and multi-component radial distribution function
506 calculation method, which predict the mixing and separation behavior of particles in

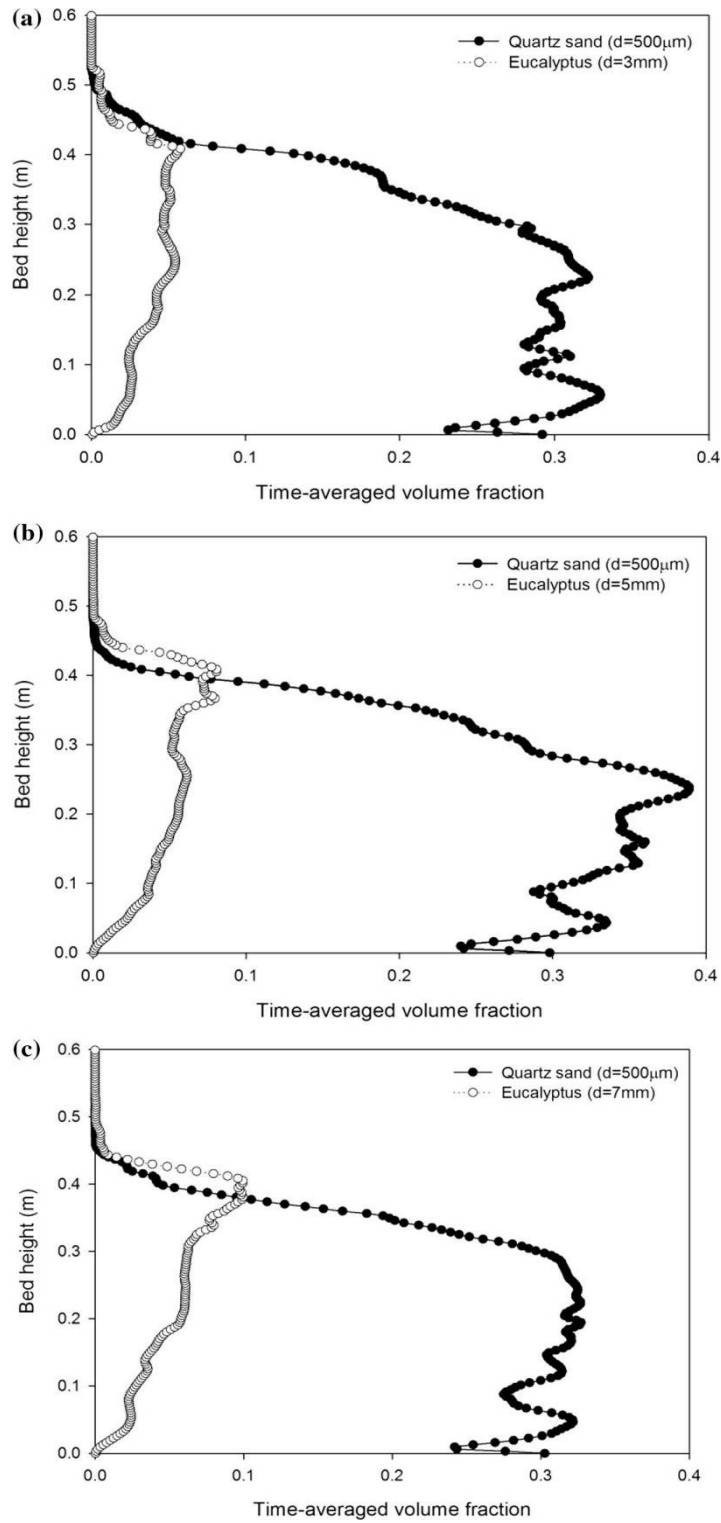
507 the fluidized bed accurately. Tang et al. (Tang, 2016) studied the numerical simulation
508 of the fluidization characteristics of the multi-component particles in circulating
509 fluidized bed. From the research, It can draw conclusions that the concentration
510 distribution pattern does not appear different due to different particles. Although the
511 distribution of fine particles in the hearth is also consistent with the trend of thinning
512 and thickening, it is more uniform than the other two kinds of particles. The medium
513 particles are mainly distributed in the middle and lower sections, and a high
514 concentration of particles accumulates at the bottom slope. However, the shape of the
515 particle distribution region is the same as that of other particles, and the coarse particles
516 show a significant difference in concentration, and they are gathered at the bottom of
517 the furnace to the secondary air. Cardoso et al. (Cardoso et al., 2018) studied the effects
518 of particle size and density of three different biomasses and sand on particles mixing
519 and separation. Fig. 10 and Fig. 11 show the distribution patterns relating the
520 density and size effect in mixing and segregation, along the bed height, for the binary
521 mixture of quartz sand and the three biomass species, respectively. The results of the
522 simulation study indicated that mixing and segregation differences among the two
523 granular species depend on the density and size ratio effect of the biomass-sand mixture,
524 where the physical differences regarding the two species contribute to the solids
525 distribution in the bed. Cardoso et al. (Cardoso et al., 2018) studied 2D and 3D
526 numerical simulations to predict the behavior of the entire gasification process in a
527 bubbling fluidized bed reactor. The effect of density difference of quartz sand and the

528 three-biomass species on particle mixing and separation was studied in Fig. 12. The
529 yellow shaded area points the level of biomass segregation at the bed top. Both 2D and
530 3D time-averaged density profiles show that the lighter biomass, balsa wood (137
531 kg/m³), revealed higher segregation at the bed top. When the density of biomass
532 particles increases, both models show a weakening of the separation effect between
533 particles, and the mixing behavior tends to increase to some extent.



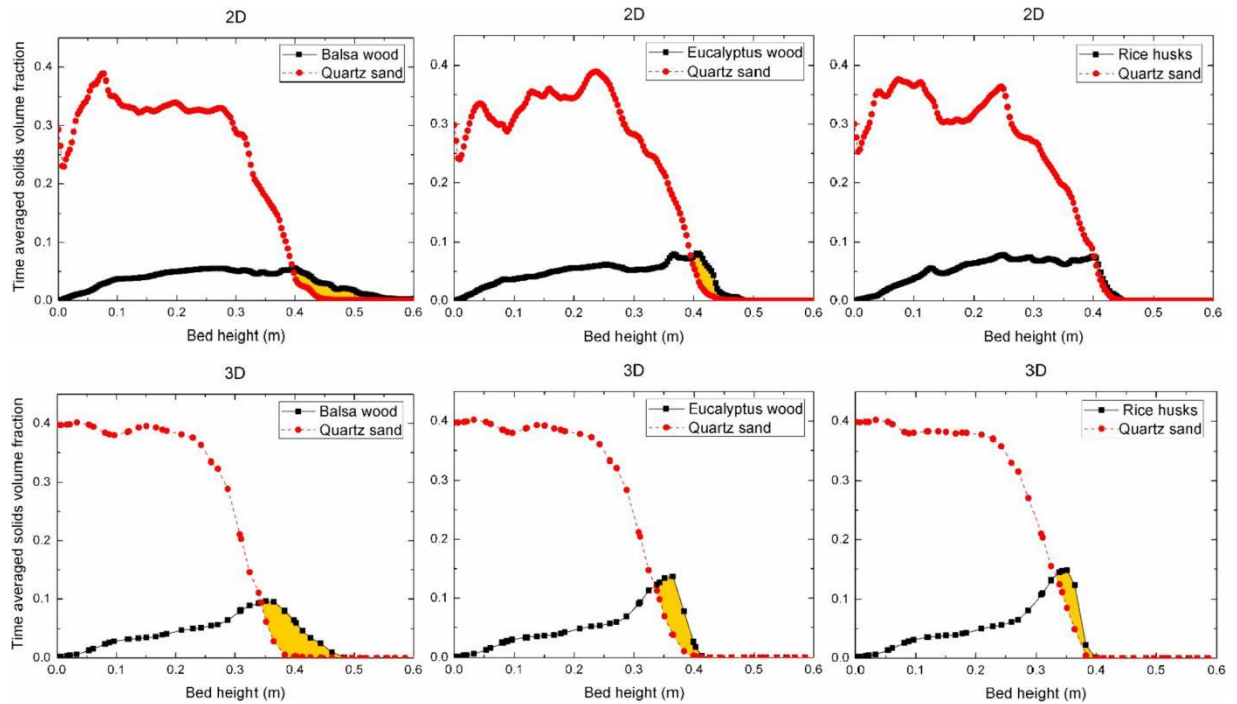
534

535 **Figure 10:** Density comparison between quartz sand and the three tested biomass substrates volume
 536 fractions along the bed height, measured by means of a vertical centerline. (a) balsa wood
 537 ($\rho = 137 \text{ kg/m}^3$); (b) eucalyptus ($\rho = 478 \text{ kg/m}^3$); (c) rice husks ($\rho = 950 \text{ kg/m}^3$); ($t = 3 \text{ s}$) (Cardoso
 538 et al., 2018).



539

540 **Figure 11:** Size comparison between quartz sand and three different eucalyptus particle size volume
 541 fractions along the bed height, measured by means of a vertical centerline. (a) deuca=3mm; (b)
 542 deuca=5mm; (c) deuca=7mm; (t=3s). (Cardoso et al., 2018).



543

544 **Figure 12:** Density effect on mixing: 2D and 3D time-averaged solids volume fraction comparison
 545 between quartz sand and the three biomasses tested (balsa wood, eucalyptus and rice husks) gathered
 546 at the reactor's centreline. (Cardoso et al., 2019).

547 **4 EFFECT OF THE GAS VELOCITY**

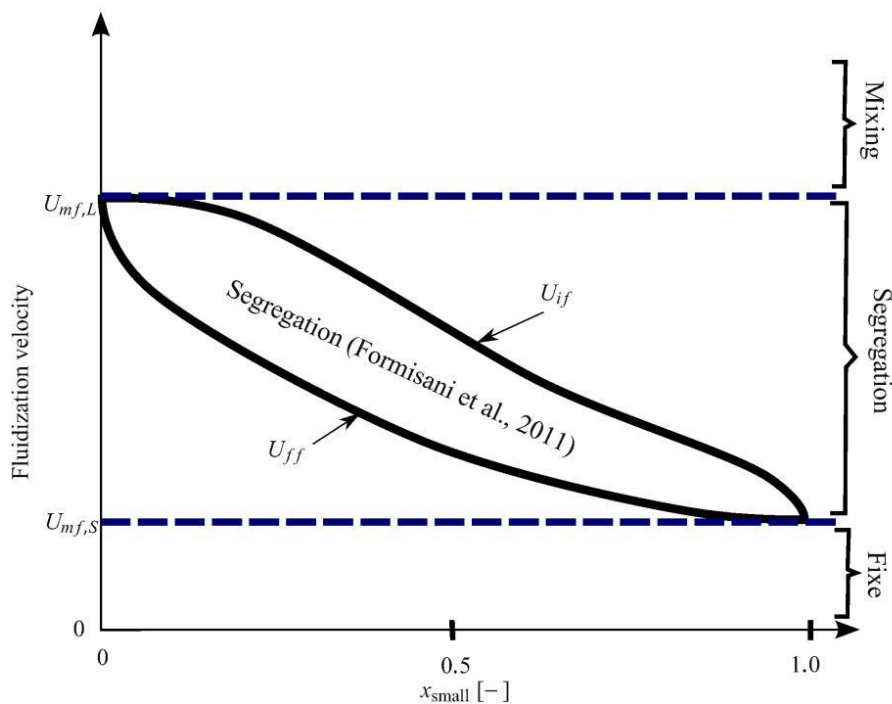
548 The difference in gas flow rate will have an important effect on the mixing and
 549 separation of particles when the fluidized bed is composed of various particles with
 550 different diameters or densities, and there will be three typical particle mixing and
 551 separation states due to the gas velocity in Figure 13. In the three states, the first state
 552 is that when the air velocity is low, the particles are completely separated. The second
 553 state is when the gas velocity is moderate; the particles are partially separated and
 554 partially mixed. Finally, the particles are presented at high gas velocity, and they
 555 eventually reach the complete mixing stage. The minimum fluidization speed has a
 556 great influence on the movement of the particles. At present, for the minimum

557 fluidization velocity of multi-component particles, the experimental value is generally
 558 fitted to determine the minimum flow of the mixture. The speed curve, and finally draw
 559 an empirical formula to predict the value. Mohammad Asif summarized and classified
 560 detailed calculation methods for minimum fluidization velocity under various
 561 conditions based on previous experience. For mixed-grained fluidized-bed with
 562 different properties and multi-component particles, a hybrid particle system was
 563 proposed. The minimum fluidization speed formula as follows:

564
$$\frac{1}{\sqrt{U_{mf}}} = \sum_1^n \frac{X_i}{\sqrt{U_{mfi}}}$$

565 (3)

566 Many researchers at home and abroad have studied the effect of gas velocity on the
 567 mixing and separation of particles.



568

569 **Figure 13:** Diagram of the fluidization patterns of binary mixture system. Formisani et al.
570 (Formisani et al., 2011) shows a density-based binary mixture: U_{if} is the initial fluidization and U_{ff}
571 refers to the velocity at which fluidization state is achieved. $U_{mf,S}$ and $U_{mf,L}$ denote the minimum
572 fluidization velocities of the small and large particles, respectively. (Konan and Huckaby, 2017)
573 (Gera et al., 2004).

574 More studies (Sharma et al., 2014a) (Cardoso et al., 2019) (Lu et al., 2003b) have shown
575 that in multi-component fluidized bed systems, at low gas velocities, particles of
576 different compositions exhibit a separation state, and at higher gas velocities, uniform
577 mixing phenomena are exhibited. Cardoso et al. (Cardoso et al., 2019) studied 2D and
578 3D numerical simulations to predict the behavior of the entire gasification process in a
579 bubbling fluidized bed reactor. In order to evaluate the effect of superficial gas velocity
580 on mixing in 2D and 3D configurations, four different inlet velocities were practised
581 (0.15, 0.25, 0.4 and 0.6 m/s) and presented in Figure 14. Results show that higher
582 superficial gas velocities (0.6 m/s) presented improved mixing ability (higher mixing
583 index), while for the lower velocities (0.15 m/s) the trend changed providing a
584 diminished mixture (lower mixing index). Concerning the superficial gas velocity effect
585 on the mixture, the 2D and 3D profiles show a reasonable agreement. In addition, some
586 literature indicates that gas velocity has a more sensitive effect on the mixing and
587 separation of particles. Jinsen Gao et al. (Gao et al., 2009) showed that binary mixture
588 of Geldart A and D particles with the gas velocity range of 0.2-0.7 m/s was researched
589 in their simulations. The results show that at low gas velocity, most of the binary
590 mixtures tend to segregate. At moderate gas velocity, particles mix well in the dense
591 phase. Further increasing the gas velocity, small particles begin to accumulate in the

592 upper regime of the bed, and a segregation trend appears again. At high gas velocities,
593 segregation efficiency in the continuous classification process increases with increasing
594 the gas velocity and mean residence time of the binary mixture, however, it will occur
595 to decrease with increasing the small particle content. Chao et al. (Zhongxi et al.,
596 2012) studied the separation behavior of two types of particles with roughly the same
597 particle size and different particle densities in a dense binary gas fluidized bed using a
598 two-fluid model. Research shows that at a comparatively low superficial gas velocity,
599 the particles mainly segregate axially, and at a comparatively high superficial gas
600 velocity, the particles segregate both axially and radially.

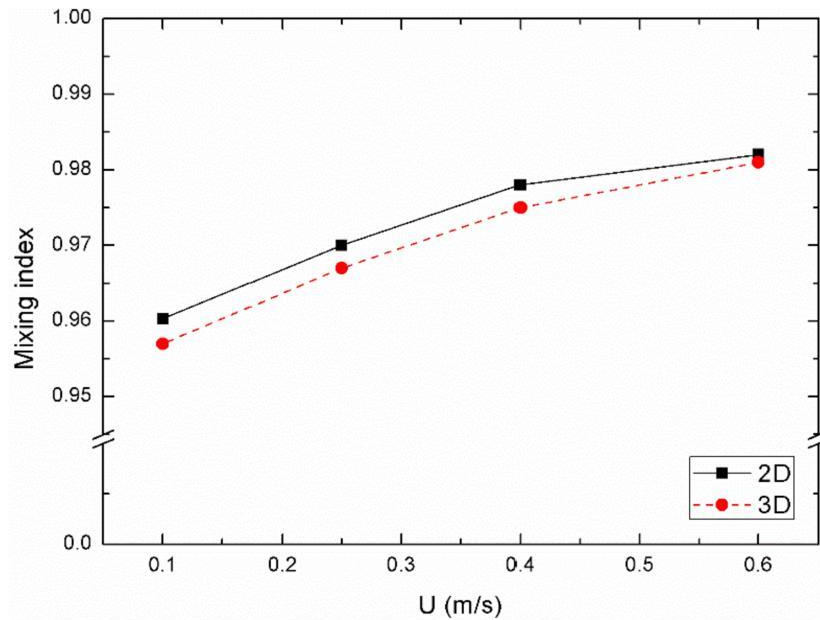
601 However, a few studies have shown that multi-component particles do not exhibit
602 segregation at low gas velocities. Gera et al. (Gera et al., 2004) extended a two fluid
603 model (gas and one granular phase) to a multi-fluid model (gas and several granular
604 phases) by adding constitutive equations for the particle-particle drag and the maximum
605 particle packing. The research reveals no segregation at low fluidization velocities,
606 segregation at intermediate velocities, and vigorous mixing at large fluidizing velocities.
607 The predicted segregation rate for a three-phase fluidized bed matches very well with
608 the measured values. Moreover, Wang et al. (Wang et al., 2009) based on the particle
609 trajectory model, and simulation of separation behavior of three-component particles in
610 fluidized bed. The behavior differences of particles at different apparent gas velocities
611 were studied. The apparent gas velocity has an important effect on the separation of
612 three-components, when the gas velocity is small, the expression of heavy constituent

613 and intermediate component particles show for jetsam and light component particles
614 show for floatsam; when the gas velocity is moderate, three compounds were separated
615 completely; when the gas velocity is large, heavy particles appear as jetsams, however,
616 light particles and intermediate particles show floatsams; when the gas velocity is too
617 large or too small, the three-components showed a completely mixed state. Lee et al.
618 (Jian and Lim, 2017) studied the Eulerian-Eulerian model and CFD-DEM applied to
619 perform simulations of solids mixing behaviors in gas fluidized beds with various inlet
620 gas velocities. Figure 16 shows the solids volume fraction profiles of solids originally
621 in the bottom section of bed at different times using Eulerian-Eulerian and CFD-DEM
622 model. The figure indicates that solids mixing behaviors simulated use Eulerian-
623 Eulerian and CFD-DEM approaches showing that significant differences could arise at
624 low inlet gas velocities. At gas velocities close to that of incipient fluidization, CFD-
625 DEM predicts higher rates of mixing than the Eulerian-Eulerian model.

626 Related studies have shown that increasing the apparent gas velocity directly affects the
627 motion state of the bubbles in the bed, which in turn affects the mixing and separation
628 behavior of the particles. Fox et al. (Rong and Fox, 2008) used a multi-fluid model to
629 research the polydisperse fluidized beds, and segregation and mixing phenomena were
630 studied for a binary system and systems with a continuous PSD. The research illustrates
631 that when the superficial gas velocity was equal to or greater than the minimum
632 fluidization velocity, more bubbles were observed in the bed, and better mixing was
633 achieved. In such case, the segregation in the bed was greatly reduced and the

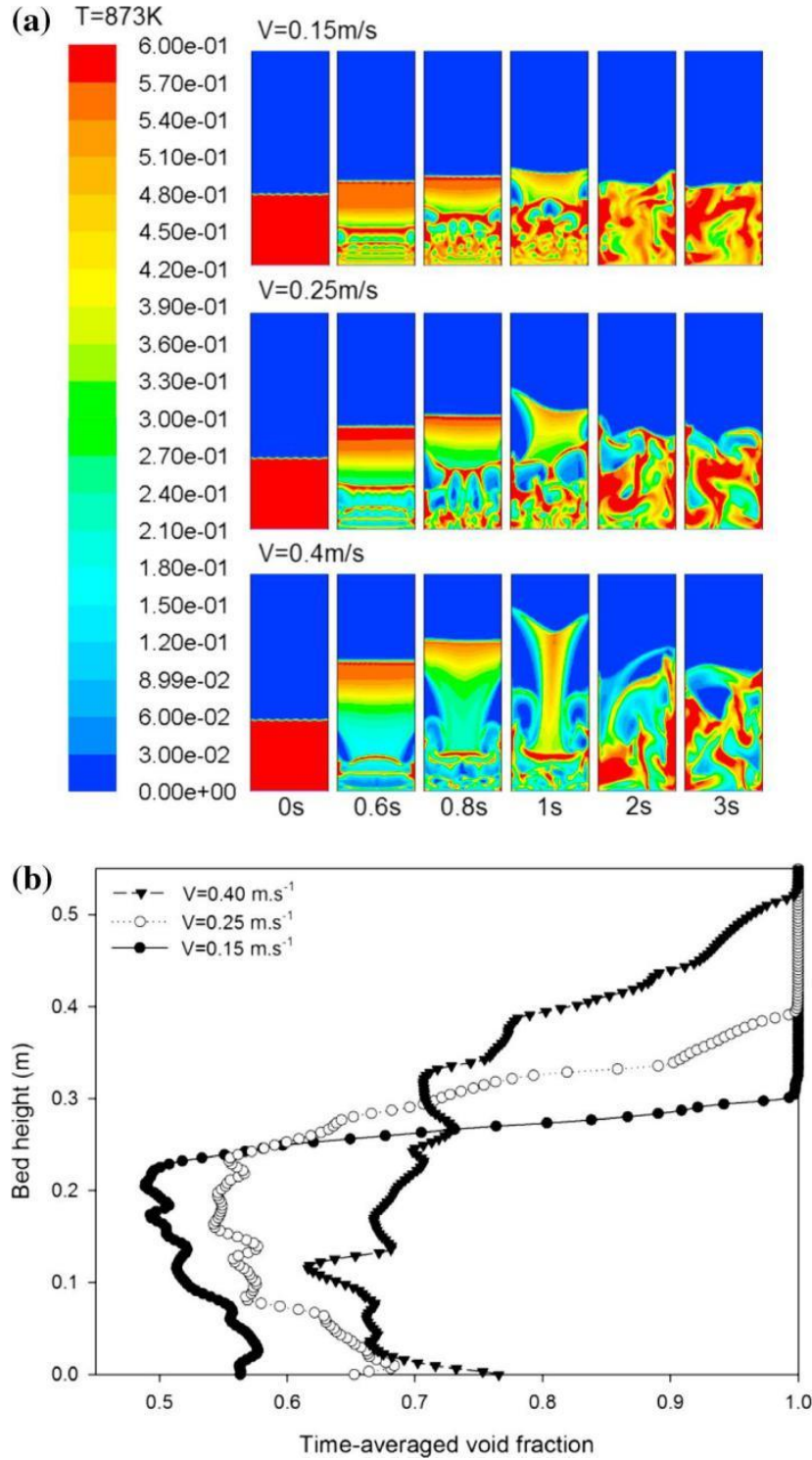
634 segregation rate was very low, around 0.1. Wang et al. (Wang et al., 2015) studied a
635 three-dimensional numerical study of the mixing and segregation of binary particle
636 mixtures in a two-jet spout fluidized bed based on Eulerian-Eulerian model. The
637 research shows that at lower jet velocities, the slip velocity between the two
638 components of binary mixtures plays a dominant role to cause the obvious segregation
639 phenomenon. However, with the jet velocity increasing, the jet penetration depth and
640 bubble amount are increased, which promotes the circulating movement of particles
641 and furthers the mixing of binary particle mixtures. Cardoso et al. (Cardoso et al., 2018)
642 studied the effect of superficial gas velocity on the mixing and separation of quartz sand
643 particles. As the velocity increases, bubbles size enlarges and grow in number and the
644 average bed height increases at different velocity ($V=0.15\text{m/s}$, 0.25m/s , 0.4m/s) in
645 Figure 15a . Such bed expansion can be reaffirmed by Figure 15b, as velocity increases,
646 more bubbles make their way to the bed surface. A higher superficial air velocity causes
647 the drag force acting on the sand particles to increase, resulting in increased particle
648 movement promoted by the augmented turbulence of the carrier air flow. The increase
649 of the superficial air velocity facilitates the mixing between the solid species with
650 different sizes and densities. Lim et al. (Lim and Lim, 2019) studied the mixing and
651 segregation behaviors of a binary mixture in a pulsating fluidized bed using the
652 Eulerian-Eulerian model. It was showed that an increase in mean inlet superficial
653 velocity of the pulsating flow increased the formation of bubbles as well as the
654 magnitudes of particle velocity within the bed. Correspondingly, there were higher

655 tendencies for particles to move upwards through the bed in the presence of more
656 bubbles and this increased mixing effects and reduced segregation between the flotsam
657 and jetsam.



658

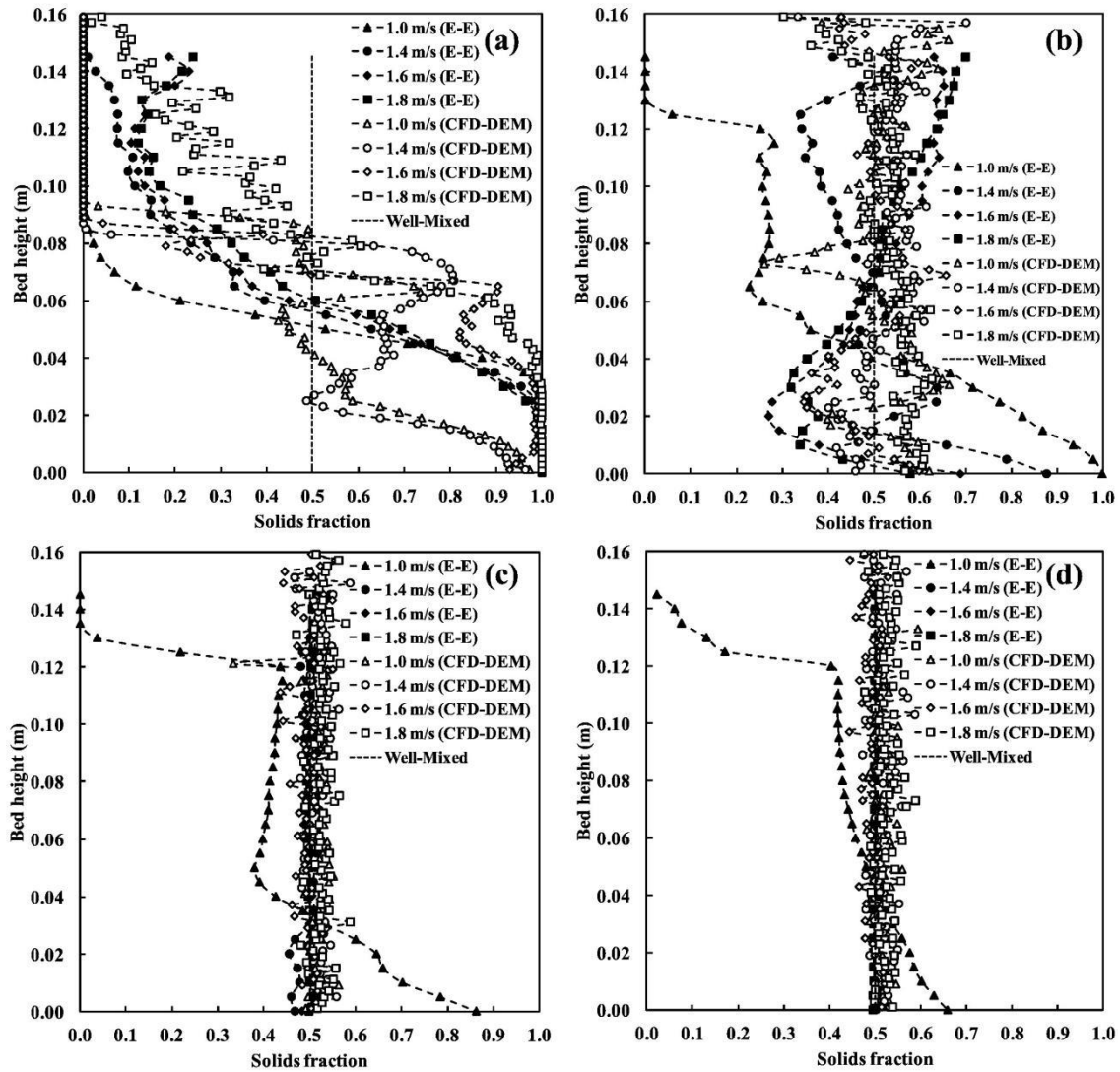
659 **Figure 14:** 2D and 3D superficial gas velocity effect on mixing. (Cardoso et al., 2019).



660

661 **Figure 15:** Superficial velocity study: (a) instantaneous contours for one granular phase (quartz
 662 sand) volume fraction at different superficial velocities (0.15m/s, 0.25m/s and 0.40m/s); (b) time-
 663 averaged void fraction along bed height at different superficial velocities (0.15m/s, 0.25m/s and
 664 0.40m/s). (Cardoso et al., 2018).

665



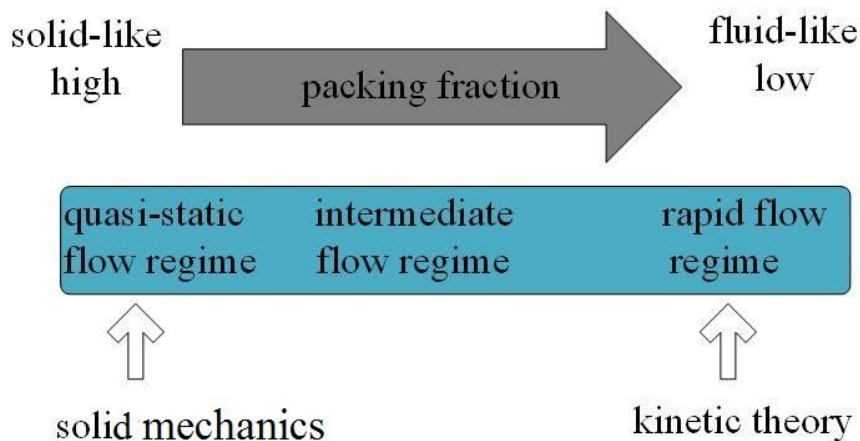
666

667 **Figure 16:** Solids volume fraction profiles of solids originally in the bottom section of bed at (a)
 668 0.5s, (b) 2 s, (c) 5 s and (d) 10 s of fluidization with various gas velocities and twice the amount of
 669 solids compared to the original setup. The profiles obtained using Eulerian-Eulerian (E-E)
 670 simulations are compared with those obtained using CFD-DEM. (Jian and Lim, 2017).

671 5 EFFECT OF THE PARTICLES FRACTION

672 It is found that not only the particle size, density and superficial gas velocity will affect
 673 the movement of particles mixing and separation, but also the proportion of different
 674 particle fractions will have some influence on them. Granular flows in particle mixer
 675 display rich behavior and may perform solid-like behavior or fluid-like behavior
 676 depending on the state of packing and the external stresses acting on the mixture as

677 schematically classified in Figure 17. The dense granular flow with very high solids
 678 packing shows a quasi-static flow regime. The frictional stress predominates between
 679 particles and the granular behavior therein is quite well modeled by soil mechanics (Luo
 680 et al., 2013). When the solids packing is very low, the dilute granular flow may show a
 681 rapid flow regime.



682

683 **Figure 17:** Schematic representation of different flow regimes of granular flow under different
 684 packing conditions. Soil mechanics and kinetic theory are frequently used models for the study of
 685 quasi-static granular flow and rapid granular flow, respectively. (Huang and Kuo, 2014).

686 Some scholars have studied the effects of different particle components on the mixing
 687 and separation of particles. Most studies have shown that the composition of solid
 688 particles has a certain effect on the mixing and separation of particles. Lu et al. (Lu et
 689 al., 2003b) studied the separation effect of particles with different sizes in a bubbling
 690 fluidized bed by experiments and numerical simulations. The results show that the
 691 mixed flow behaviors of two kinds of particles with the same density and different
 692 particle size are mainly caused by the difference of the average particle size and the
 693 mass fraction of the particles. In addition, the study found that the proportion of small

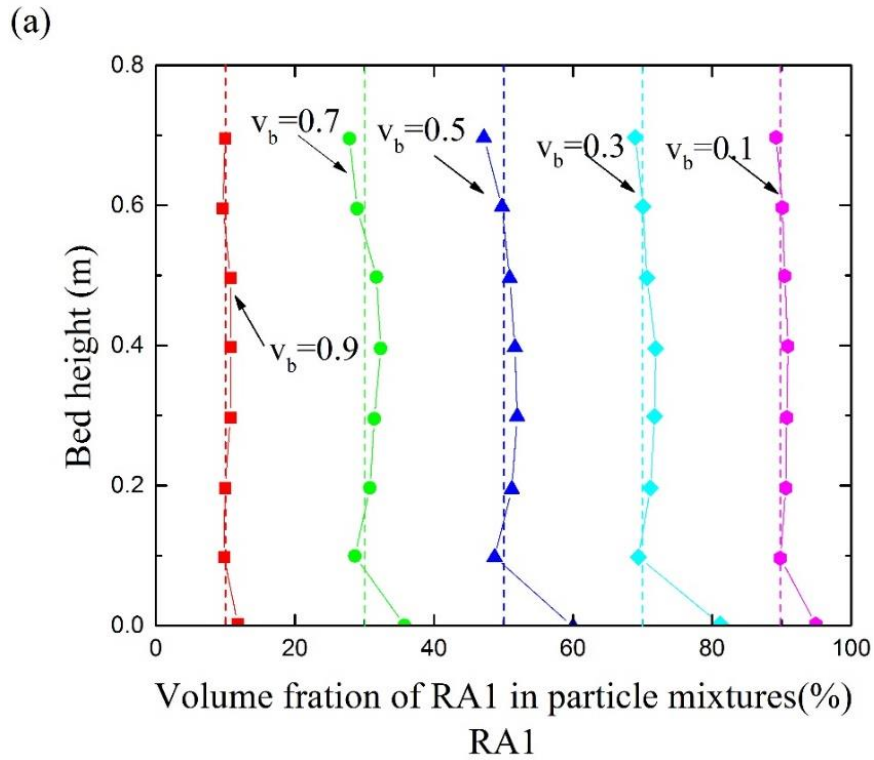
694 particles is the key factor of particle separation. The reason for this phenomenon is that
695 the initial fluidization state of the binary mixture is characterized by a total pressure
696 drop equal to the minimum fluidization velocity of the particle weight per unit area of
697 the bed, which depends on the average mass fraction of small particles. Gao et al. (Gao
698 et al., 2009) studied the mixing and separation of Geldart A and B particles by
699 experiment and numerical simulation. The study found that the mixing trend of binary
700 mixtures increased with the increase of small particle content at a high gas velocity. The
701 phenomenon occurs because the addition of small particles affect the flow of gas
702 through the dense phase of the fluidized bed, producing smaller bubbles and resulting
703 in smoother fluidization. In addition, the study also found that as the mass fraction of
704 small particles increases, a large number of smaller bubbles are produced, causing more
705 particles in the dilute phase. Therefore, the mixing of small particles and large particles
706 is improved. Wang et al. (Wang et al., 2015) based on the Eulerian-Eulerian model, and
707 the mixing and separation process of two-component particles in a double nozzle
708 spouted bed was studied under three-dimensional conditions. Figure 18 shows the
709 volume fraction variations of binary particle mixtures along with the bed height under
710 different initial mixture compositions with a constant jet velocity ($u_{jet} = 35u_{uff}$). It is
711 found that when two kinds of particles are according to the equivalence ratio, they can
712 achieve the best separation effect; as the ratio become larger, the two kinds of particles
713 mixture well because the system is close to single particle state at this time.
714 Mostafazadeh et al. (Mostafazadeh et al., 2013) used the Eulerian-Eulerian model

715 coupled with the kinetic theory of granular flow to study the two-dimensional gas-solid
716 fluidized bed reactor. Figure 1 shows that as the mass fraction of small particles
717 increases, more particles are entrained into the dilute phase, resulting in a decrease in
718 the average diameter of the mixture and an increase in bed height. In addition, when
719 the mass fraction of larger particles increases, the average diameter of the mixture in
720 the bed increases while bed height decreases. Du et al. (Wei et al., 2016) studied on the
721 effect of mixing ratio on segregation with binary mixtures of A1 (Geldart-B) particle as
722 the primary particles and S1 (Geldart-D) particles as the coarse particles. The mixing
723 ratios of A1: S1 were set at 1:1, 1:2 and 2:1, respectively. The simulation results showed
724 that by increasing the proportion of coarse particles, mixing between particles can be
725 suppressed, and the stability of the bed can be improved. Sant'Anna et al. (Sant'Anna et
726 al., 2016) studied the numerical simulation using CFD of a gasifier bubbling fluidized
727 bed for the system composed of gas-biomass-sand. The simulations show that
728 segregation of the particulate medium occurred for assays where the ratio between the
729 mass of each biomass particle and the mass of each sand particle was > 1.0 coupled to
730 a ratio between biomass and sand volume fractions in the bed ≤ 0.5 .

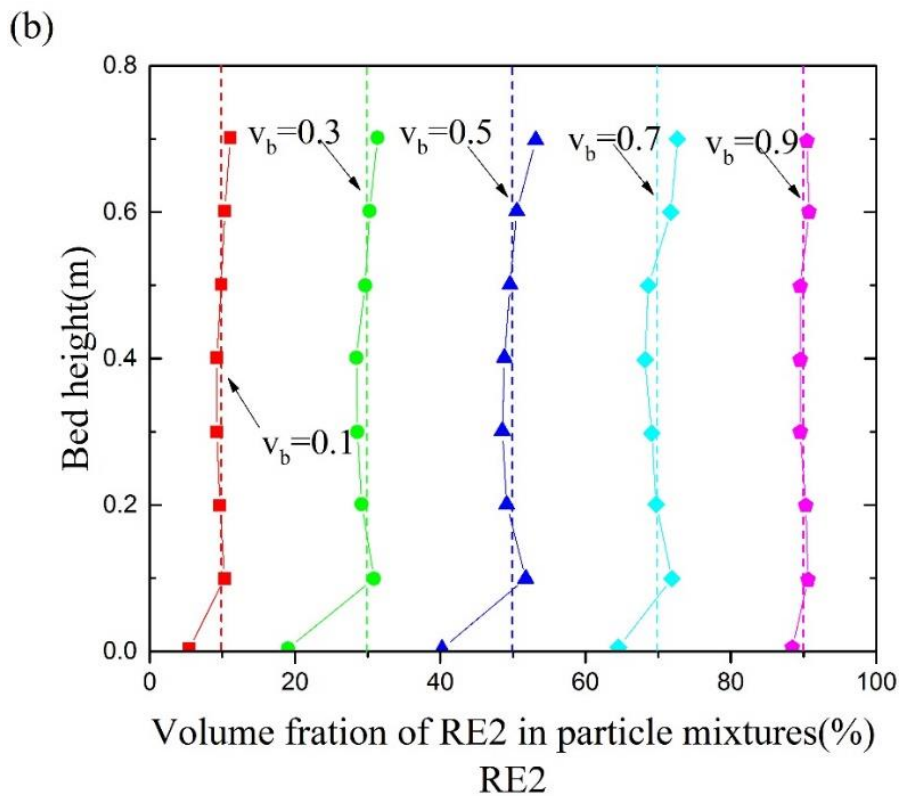
731 Wei et al. (Wei et al., 2019) extended a particle-particle (p-p) drag model to cohesive
732 particle flow by introducing solid surface energy to characterize cohesive collision
733 energy loss. The effects of the proportion of cohesive particles on the mixing of binary
734 particles were numerically investigated with the use of a Eulerian multiphase flow
735 model incorporating the p-p drag model. The study shows that cohesive particle

736 proportions greatly affect the mixing index of binary particles and optimal mixing was
737 observed with an increase of the cohesive particle proportion at a certain superficial
738 velocity.

739 However, some studies have shown that the composition ratio of the particles has little
740 effect on the mixing and separation of the particles. Cooper et al. (Cooper and Coronella,
741 2005b) investigated the parameters of maximum packing fraction for the relative effects
742 on bubbling and hence on particle mixing and segregation. The results indicates that
743 maximum packing fraction, and the composition ratio of the solid mixture does not
744 affect the extent of mixing. Fotovat et al. (Fotovat et al., 2015) used different
745 experimental techniques and an Eulerian n-fluid approach in the work to shed light on
746 the fluidization and mixing characteristics of large biomass particles fluidized with sand
747 under the bubbling conditions. Figure 20 presents the time-average axial profile of the
748 normalized mass of biomass for mixtures composed of 8 wt% and 16 wt% biomass. A
749 satisfactory level of consistency is observed between the numerical results and
750 experimental measurements. Studies have shown that the difference in mass fraction of
751 biomass particles has no significant effect on particle mixing and separation, and in
752 both cases, the overall movement tendency of the particles in the bed is consistent.

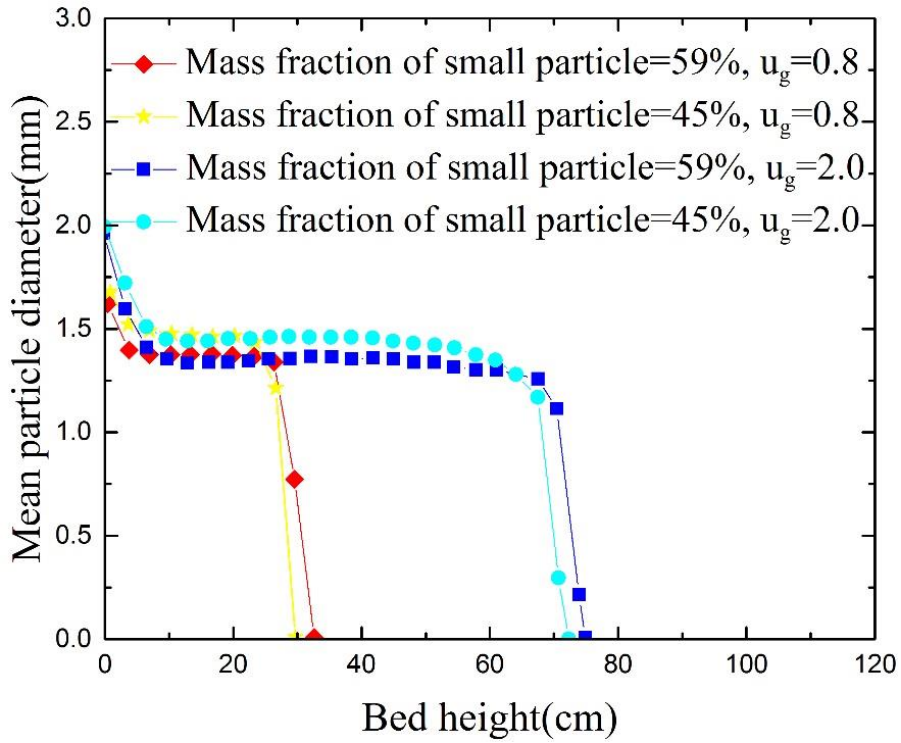


753



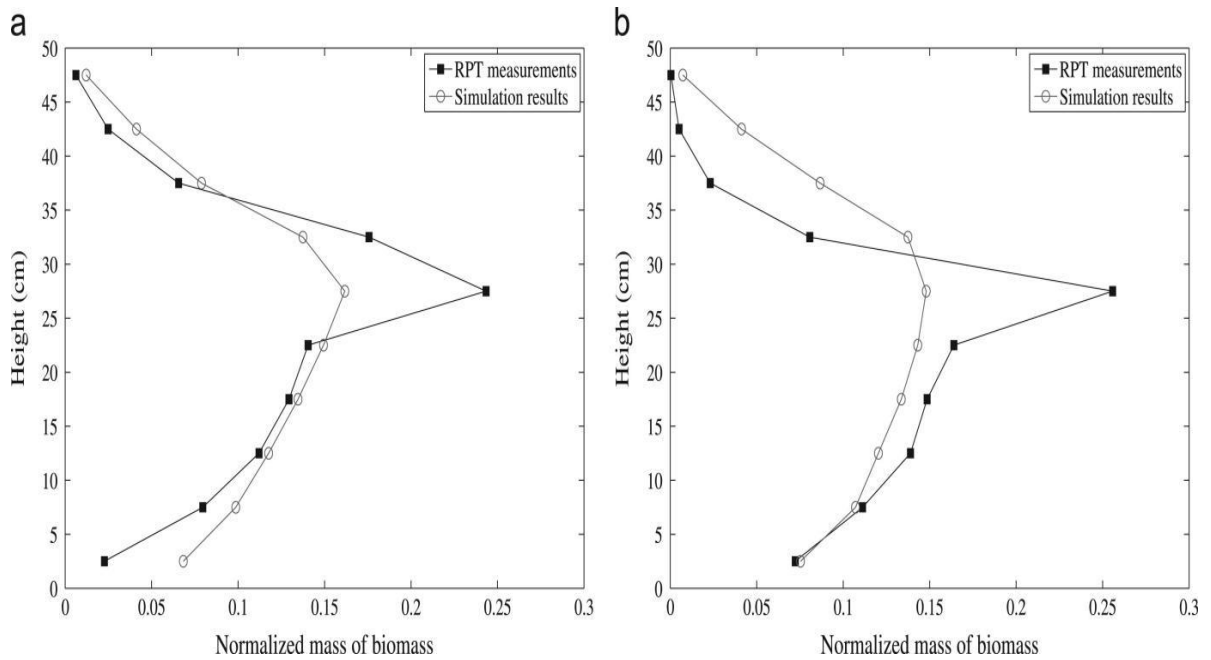
754

755 **Figure 18:** Volume fraction variations of binary particle mixtures with the bed height under different
 756 initial mixture compositions. (Wang et al., 2015).



757

758 **Figure 19:** Bed average diameter for various compositions of the mixture. (Mostafazadeh et al.,
759 2013).



760

761 **Figure 20:** Comparison between (a) the RPT experimental measurements and (b) 3-D numerical
762 simulation of the axial profile of the normalized mass of biomass. ($U/U_{mf,s}=4$). (Fotovat et al.,
763 2015).

764

765 **6 EFFECT OF MODEL PARAMETRES**

766 It is found that the selection of some important parameters in the model have an
767 important effect on the multi-particles mixing and separation. Some scholars have
768 studied the influence of some modeling parameters (including the expression of solid
769 viscosity, recovery factor and particle temperature equation) on predicted
770 mixing/segregation behavior or the combined effect of these parameters.

771 **6.1 Effect of Particle-Particle Restitution Coefficient and Particle-** 772 **Particle Friction Coefficient**

773 The inelastic collision is considered by the recovery coefficient and friction coefficient.
774 The lower e_{pp} means more energy loss due to particle-particle collisions. In general, an
775 accurate measurement of the recovery coefficient is often difficult because its value
776 depends not only on the properties of the material but also on the speed of the relative
777 collision. Adjustment parameters generally used as the result of the matching
778 experiment. Some researchers have done numerous research on related aspects.

779 In the early days, some scholars mainly conducted qualitative research on the particle-
780 particle restitution coefficient. Liu et al. (Liu et al., 2003) based on particle dynamics
781 and gas-solid two-phase fluid dynamics, and a hard-ball simulation method was used
782 to study the interparticle collision. It has been found that the coefficient of elastic
783 recovery of granule affects the flow structure of two-component particles of equal
784 diameter and non-density, especially the separation effect between particles.

785 Specifically, under non-elastic collision conditions, the heavy particles will be carried
786 to the surface of the bed under the action of upward moving bubbles. On the other hand,
787 due to their own gravity, the particles will drop and settle on the bottom of the bed. The
788 case is easier to separate between the particles. Under the elastic collision condition,
789 bubbles are hardly formed because the energy loss between the particles is not
790 considered, and the effect of particle deposition is not obvious, which is not conducive
791 to the separation between the particles. Zheng et al. (Zheng and Liu, 2010) based on
792 two-fluid flow model combining with the kinetic theory of granular flow, considering
793 the effect of restitution coefficient of particle elasticity to the interaction and
794 dissipations of fine particles. The simulation results show that the influence of
795 restitution coefficient of fine particles on the fluidization characteristics in the bed can
796 not be neglected. As the restitution coefficient between the particles increases, the
797 collision between the particles becomes more intense, the size of the agglomerates of
798 the particles becomes uniform, and the mixing of the particles in the fluidized bed is
799 more uniform.

800 In recent years, more scholars have quantitatively studied the effect of particle-particle
801 restitution coefficient on particle mixing and separation, and obtained the choice of
802 values in specific cases. 3D Computational Fluid Dynamics simulation of a gas-solid
803 bubbling fluidized bed was performed to investigate the effect of restitution coefficient
804 on particle motion behavior by Esmaili et al. (Esmaili and Mahinpey, 2011b). The
805 literature uses adjusted Di Felice drag model for seven different restitution coefficients

806 ($e_{pp}=1, 0.99, 0.97, 0.95, 0.9, 0.8, 0.7$) proposed for simulation of fluidized beds.

807 As collisions become less ideal (and more energy is dissipated due to inelastic collisions)

808 particles become closely packed in the densest regions of the bed, resulting in sharper

809 porosity contours and larger bubbles. Sharma et al. (Sharma et al., 2014a) reported the

810 restitution coefficient of biomass and bio-char particles affects the mixing/segregation

811 behavior of the solid phases in the bubbling fluidized bed. It is shown that with the

812 increase of restitution coefficient, there is a decrease in pinewood mass fraction (%) in

813 the lower region of the bed, while there is an increase in mass fraction (%) in the upper

814 region of the bed. However, the more precise impact still needs further in-depth research.

815 Ebrahim et al. (Azimi et al., 2015) studied how to improve the accuracy of numerical

816 simulation in predicting particle mixing and separation by simulating two-component

817 particles in two-dimensional and three-dimensional systems under different conditions.

818 The study found that the accuracy of the simulation under the three-dimensional system

819 is higher than that of a two-dimensional system. When the recovery coefficient between

820 particles is taken as 0.9, the accuracy of numerical simulation to predict particle mixing

821 and separation can be effectively improved. Geng et al. (Geng et al., 2016) studied the

822 hydrodynamics of binary coal-sand mixture in a pseudo-2D rectangular bubbling

823 fluidized bed simulated and use the multi-fluid model incorporating the kinetic theory

824 of granular flow. In the study three different values of e_{pp} (0.7, 0.8, and 0.9) were

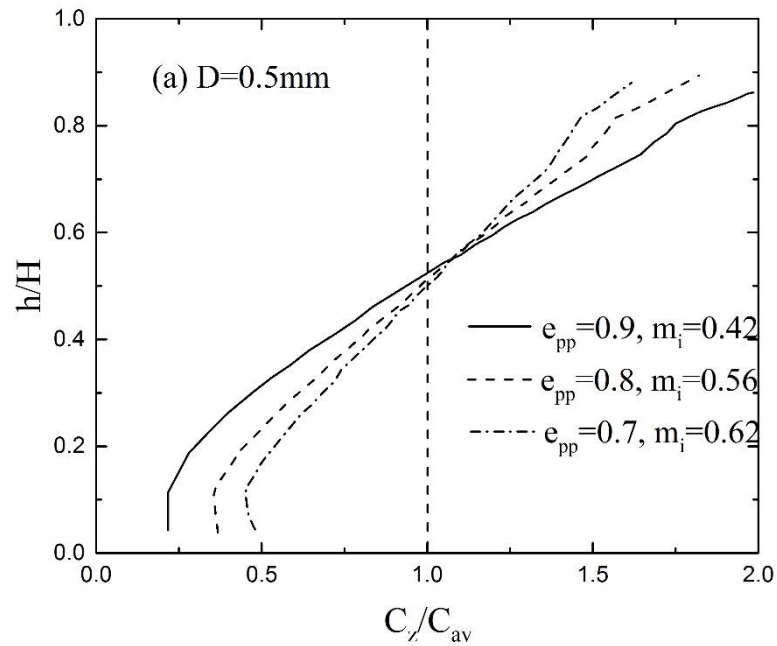
825 examined, the results of the study are shown in Figure 1. The study found that when the

826 bed depth was equal to 20 mm, the influence of e_{pp} on particle axial mixing behavior

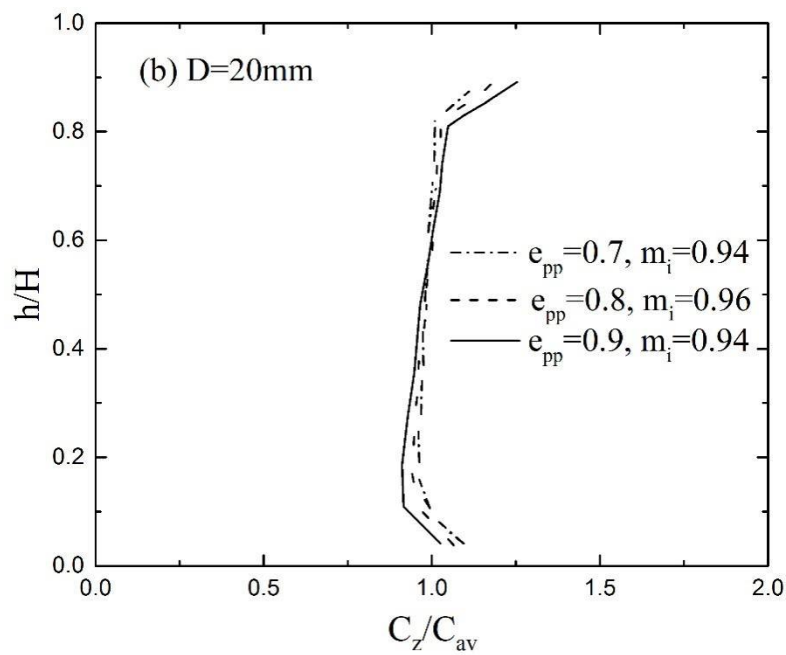
827 was unimportant. However, for the bed with a depth of 5 mm, the axial segregation is
828 strengthened with the increase of e_{pp} . Moreover, the best agreement with the
829 experimental data was achieved when e_{pp} is equal to 0.9. However, A small number of
830 scholars have shown that the coefficient of restitution between particles does not affect
831 the mixing and separation of particles. Tagliaferri et al. (Tagliaferri et al., 2013) studied
832 the values investigated for the restitution coefficient were 0.60, 0.70, 0.80, 0.90 and
833 0.99. The research shows that the value selected for the restitution coefficient does not
834 affect the numerical results significantly, except for $e=0.99$.

835 Because the study found that the coefficient of friction between the particles has little
836 effect on the system, only a small amount of literature is organized here. Zhong et al.
837 (Zhong et al., 2014a) studied the effect of particle-particle friction coefficient on the
838 mixing and separation behavior of particles in a bubbling fluidized bed based on the
839 Eulerian-Eulerian model. The two solid particles studied in the literature have different
840 densities and sizes. The results show that when modeling the segregation process at low
841 gas velocity, both axial and radial jetsam velocities decrease with the increase of the
842 particle-particle friction coefficient. The simulation with a small particle-particle
843 friction coefficient overestimates the degree of segregation, and the good quantitative
844 results are obtained when the particle-particle friction coefficient is 0.3. And the study
845 found that the mixing effect of particles is not affected by the friction coefficient.
846 Although the value of 0.15 was used in some literature (Gera et al., 2004, Rong and
847 Fox, 2008, Mazzei et al., 2010), the particle-particle friction coefficient was generally

848 set to 0, which meant that the particle frictional sliding effect during collisions.



849



850

851 **Figure 21:** Coal concentration profiles for different solid-solid restitution coefficients of (a)
852 D=5mm, and (b) D=20 mm beds. (Geng et al., 2016).

853 6.2 Effect of Wall Boundary Condition

854 The interactions between wall and particles are also critical for the accurate prediction

855 of the complex hydrodynamics in fluidized beds. (Li et al., 2010) Generally, the

856 Johnson and Jackson (Johnson and Jackson, 1987) wall boundary condition is applied
857 in the CFD simulations of gas-solids flow. This wall boundary condition includes two
858 important parameters, the specular coefficient, ϕ , which characterizes the tangential
859 momentum transfer from the particles to the wall and the particle-wall restitution
860 coefficient, e_{pw} . The specular coefficient is an important parameter in the phase
861 condition of Johnson-Jackson particle phase wall. For $\phi = 0$, a free-slip boundary
862 condition without frictional effect of particles on the wall is applied, while for $\phi = 1$, a
863 no-slip boundary condition with frictional effect of particles on the wall is employed.
864 And no-slip (Gao et al., 2009, Coroneo et al., 2011) or partial-slip (Lu et al., 2003b, Lu
865 et al., 2007b, Benyahia, 2008, Mathiesen et al., 2010) wall boundary condition has been
866 applied in the numerical investigation of bed hydrodynamics of binary particle mixtures.

867 Some scholars have done research in this area. Some literatures have qualitatively
868 studied the effect of the specular coefficient on the mixing and separation of multi-
869 component particles. Lungu et al. (Lungu et al., 2015) investigated the effect of
870 specular coefficient on the flow characteristics of two-component particle mixture
871 using a simplified two-dimensional simulation system. The specular coefficient, ϕ is
872 observed to have considerable effect on the axial mixing in the fluidized bed. The
873 mixing index reduces sharply with increasing values of the specular coefficient for
874 the two drag models (Gidaspow and EMMS models) eventually becoming constant at
875 $\phi = 0.05$. Zhong et al. (Zhong et al., 2016) in order to reveal the fluidization
876 characteristics of binary particles, the 3D computational fluid dynamics (CFD)

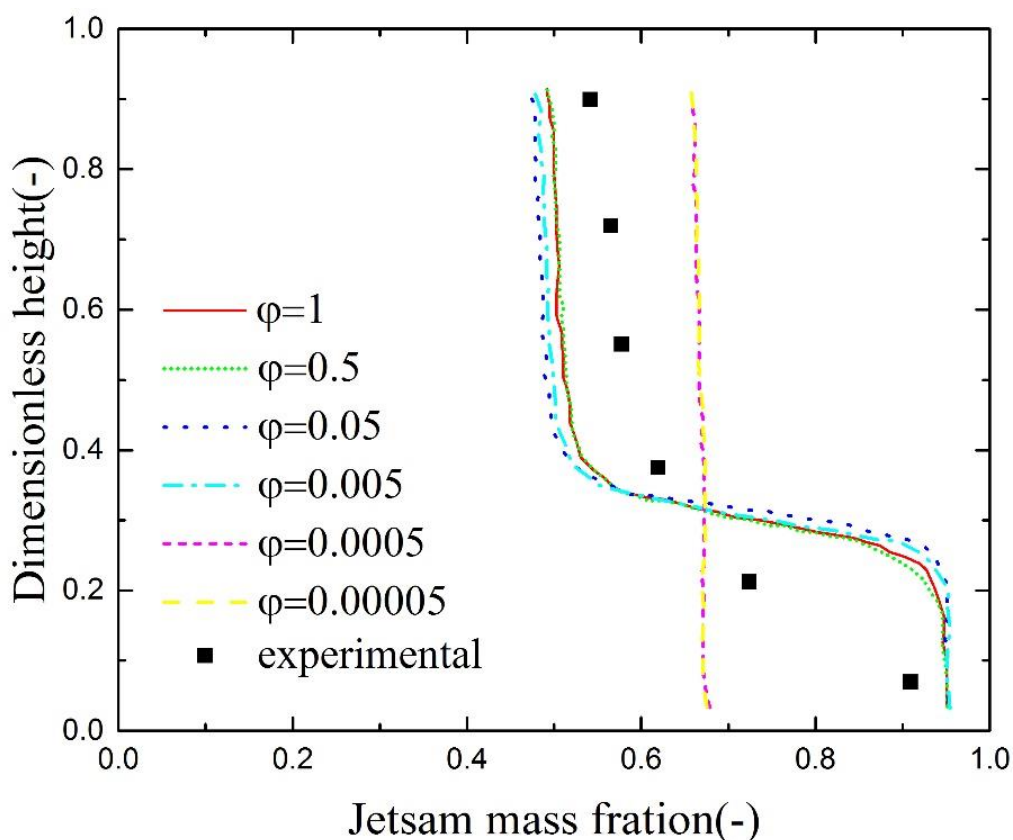
877 simulation on the instantaneous segregation process of binary particles in gas-solid
878 fluidized bed was performed using the multi-fluid model based on Eulerian-Eulerian
879 method. The study investigated the effect of specular coefficient on the three-
880 dimensional CFD simulation results of transient grading process. As the specularity
881 coefficient decreases, the degree of temporal grading predicted at the same time is
882 significantly reduced. When the specularity coefficient is 0, the full-slip wall condition,
883 even after the classification is completed, the classification degree of the large and small
884 particles in the system is still very small, which is close to the state of complete mixing.
885 A reduction in the specularity coefficient will hinder the classification behavior of the
886 two-component particle mixture and enhance the mixing behavior of the system. Geng
887 et al. (Geng et al., 2016) studied the boundary wall condition to investigate the influence
888 on the predicted particles mixing/segregation behavior. To research the influence of
889 specularity coefficient, the sand and coal particles and five different specularity
890 coefficient values ($\varphi = 0, 0.005, 0.05, 0.5, 1.0$) were performed. It can be found that the
891 predicted mixing degree decreased with the increase of specularity coefficient. The best
892 agreement between simulation results and experimental data was achieved when
893 specularity coefficient was equal to 1.0.

894 Quantitative effects of specularity coefficient on particle mixing and separation have
895 been reported in related literatures. Zhong et al. (Zhong et al., 2012) investigate the
896 influence of wall boundary condition on the predicted segregation and mixing behavior.
897 They found that the predicted segregation is significantly affected by the specularity

898 coefficient for the segregation process. However, it effects lightly on the mixture and
899 no segregation can be predicted for small specularly coefficients. The axial segregation
900 profiles for different specularly coefficients are shown in Figure 22. As we can see
901 from the figure, the degree of segregation increases obviously when the specularly
902 coefficient decreases from 0.5 to 0.05. However, when the specular reflection
903 coefficient is smaller than 0.05, the particles will have a better mixing. This is because
904 when the mirror coefficient is too small, it means that the friction between the particles
905 and the wall surface can be neglected, so the separation effect between the particles is
906 not obvious. Recently, Sharma et al. (Sharma et al., 2014a) reported that the variation
907 of mixing degree versus specularly coefficient was not monotonous. It was found in
908 high velocity when the specularly coefficient is 0.5 the pinewood and bio char particles
909 segregation was clearly observed. However, when the specularly coefficient is 0 or 1,
910 the solid particles mixture well. Bakshi et al. (Bakshi et al., 2015) modeled the
911 hydrodynamics of dense-solid gas flows strongly affected by the wall boundary
912 condition and in particular, the specularly coefficient ϕ . Comparison of simulation
913 predictions with experimental data for different fluidization regimes and particle
914 properties suggests that values of ϕ in the range [0.01,0.3] are suitable for simulating
915 most dense solid-gas flows of practical interest.

916 In the numerical simulation of multi-component particle mixing and separation systems,
917 the setting of the particle-wall restitution coefficient is less important than the
918 specularly coefficient. Zhong et al. (Zhong et al., 2012) studied the $e_{pw}=0.9$ and 0.99,

919 and found that the particle-wall restitution coefficient only plays little role in predicting
 920 the segregation and mixing of binary particle mixtures in bubbling fluidized beds,
 921 which is consistent with the previous work shows that the particle-wall restitution
 922 coefficient plays only a minor role in numerical modeling of bubbling fluidized beds
 923 (Li et al., 2010), CFB risers (Almuttahir and Taghipour, 2008), and spouted beds (Lan
 924 et al., 2012). And Enyahia et al. (Benyahia et al., 2005, Almuttahir and Taghipour,
 925 2008, Wang et al., 2010) proposed to calculate the hydrodynamic behavior in a fast
 926 fluidized bed using the small wall reflection coefficient.



927

928 **Figure 22:** Axial segregation profiles for different specular coefficients for $U_g=0.0384$ m/s
 929 ($e_{pw}=0.90$). (Zhong et al., 2012).

930

931 **7 OUTLOOK**

932 The study on the mixing and separation of multi-component particles in a fluidized bed
933 by the Eulerian-Eulerian model is instructive in practical industry. More scholars have
934 conducted important research in the regard. In most of the previous studies, the main
935 focus has been on understanding the hydrodynamics of a single solid phase in the
936 presence of a carrier gas (Shah et al., 2010, Shah et al., 2011a, Shah et al., 2011b, Shah
937 et al., 2011c)

938 Based on the extension of the two-fluid CFD models of multi-component particle
939 mixtures have been developed by some researchers, and the flow behavior of mixture
940 particles has been predicted in fluidized bed. The success of multi-fluid Eulerian
941 approach significantly depends on the proper description of inter-phase interaction
942 (Anderson and Jackson, 1967, Feng and Yu, 2007, Chao et al., 2012). For fluidized
943 particle mixture systems, special attentions have been paid to the influence of the
944 interactions between particle components on the predicted mixing behavior (Owoyemi
945 et al., 2007, Zhong et al., 2014b, Beetstra et al., 2007, Cortes and Gil, 2007). And to
946 close the governing equations for the solid phase(s), the kinetic theory of granular
947 flow(KTGF) is commonly used to provide the constitutive relations for the solid
948 phase(s). There are some studies have been based on the kinetic theory(Fan and Fox,
949 2008, Goldschmidt et al., 2001, Lu et al., 2003a, Lu et al., 2007a, Annaland et al., 2009a,
950 Annaland et al., 2009b)

951 In recent years, many scholars have studied the effects of different factors on particle
952 mixing and separation in multi-component particle systems using the method of
953 Eulerian-Eulerian. However, the current numerical simulation of gas-solid flow in a
954 fluidized bed is mostly based on the average particle properties (including particle size
955 and density) due to the limitations of the simulation conditions and the complex
956 physical properties. Most hypothetical particles are mixed and separated in a fluidized
957 bed, which greatly reduces the computational complexity and mathematical model
958 requirements. There are obvious differences in the properties of particle size and density
959 of actual bed materials. Only a simplified study of the simulation of single-component
960 particles will have a great impact on the simulation results. At present, more scholars
961 have studied the mixing and separation behaviors of two-component particles. However,
962 the mixing and separation behaviors of three-component particles have been studied
963 less. In addition, it is necessary to establish a new model to study the flow behavior of
964 three-component particles. The study of the Eulerian-Eulerian model to study the three-
965 component particles mixing and separation behavior is the urgent need for the
966 development of the project. In addition, in the study of the drag force model, researchers
967 have done some research on the drag force between gas-solid, but there are only a few
968 scholars to study the drag force interaction between multi-component particles.
969 Therefore, the study of the drag force between particles is also a major direction of
970 follow-up research.

971

972 **Notes**

973 The authors declare no competing financial interest.

974

975 **ABBREVIATIONS**

976 d_p Particle diameter

977 d_b Bubble diameter

978 u_{mf} Minimum fluidization gas velocity (m/s)

979 G Gravity acceleration (m/s^2)

980 \bar{u}_b Average velocity of bubbles

981 x_i Fluid-free volume fraction of its solid species defined as $[V_{si}/V_{st}]$

982 u_{ff} Full fluidization velocity of binary mixtures (m/s)

983 V_b Volume fraction of RE2 in particle mixtures

984 u_g Inlet gas superficial velocity

985 e_{pp} Particle-particle restitution coefficient

986 e_{pw} Particle-wall restitution coefficient

987 ϕ Specularity coefficient

988 β_{pl-ps} Large solid-small solid drag force

989 β_{g-ps} Gas-small solid drag force

990 β_{g-pl} Gas-large solid drag force

991 μ_{pl} Large solid viscosity

992 μ_{ps} Small solid viscosity

993 G_{pl} Large solid gravity

994 G_{ps} Small solid gravity

995 V_g Lift force

996 V_{pl} Large solid lift force

997 V_{ps} Small solid lift force

998

999 ACKNOWLEDGMENT

1000 The authors gratefully acknowledge financial support from the National Natural
1001 Science Foundation of China (Grant No. 51390492), A Foundation for the Author of
1002 National Excellent Doctoral Dissertation of PR China (201440) and the Fundamental
1003 Research Funds for the Central Universities. The authors also acknowledge the
1004 provision of a scholarship to Yong Zhang by the China Scholarship Council (CSC) that
1005 enabled him to carry out part of the reported work at the University of Nottingham.

1006

1007 **REFERENCES**

- 1008 Numerical Simulation of Multiphase Fluid Dynamics in Air Heavy Medium Fluidized
1009 Bed Based on Euler-Eulerian Model, China University of Mining and
1010 Technology.
- 1011 ALAM, M., T. WILLITS, J., Ö. ARNARSON, B. & LUDING, S. 2002. Kinetic theory
1012 of a binary mixture of nearly elastic disks with size and mass disparity.
- 1013 ALMUTTAHAR, A. & TAGHIPOUR, F. 2008. Computational fluid dynamics of high
1014 density circulating fluidized bed riser: Study of modeling parameters. Powder
1015 Technology, 185, 11-23.
- 1016 AND, D. L. K. & HILL, R. J. 2001. Inertial effects in suspension and porous-media
1017 flows. *Annu.rev.fluid Mech*, 33, 619-647.
- 1018 ANDERSON, T. B. & JACKSON, R. 1967. Fluid mechanical description of fluidized
1019 beds. Equations of motion. *Industrial & Engineering Chemistry Fundamentals*,
1020 6, 527-539.
- 1021 ANNALAND, M. V. S., BOKKERS, G. A., GOLDSCHMIDT, M. J. V., OLAOFE, O.
1022 O., HOEF, M. A. V. D. & KUIPERS, J. A. M. 2009a. Development of a multi-
1023 fluid model for poly-disperse dense gas–solid fluidised beds, Part I: Model
1024 derivation and numerical implementation. *Chemical Engineering Science*, 64,
1025 4222-4236.
- 1026 ANNALAND, M. V. S., BOKKERS, G. A., GOLDSCHMIDT, M. J. V., OLAOFE, O.
1027 O., HOEF, M. A. V. D. & KUIPERS, J. A. M. 2009b. Development of a multi-
1028 fluid model for poly-disperse dense gas–solid fluidised beds, Part II:
1029 Segregation in binary particle mixtures. *Chemical Engineering Science*, 64,
1030 4237-4246.
- 1031 AZIMI, E., KARIMIPOUR, S., NIKRITYUK, P., SZYMANSKI, J. & GUPTA, R.
1032 2015. Numerical simulation of 3-phase fluidized bed particle segregation. *Fuel*,
1033 150, 347-359.
- 1034 AZIZI, S., HOSSEINI, S. H., AHMADI, G. & MORAVEJI, M. 2010. Numerical
1035 Simulation of Particle Segregation in Bubbling Gas-Fluidized Beds. *Chemical
1036 Engineering & Technology*, 33, 421-432.
- 1037 BAGNOLD, R. A. 1954. Experiments on Gravity-Free Dispersion of Large Solid
1038 Spheres in a Newtonian Fluid Under Shear. *Proc.roy.soc.london*, 225, 49-63.

- 1039 BAI, D. A. S. I., ISSANGYA, A. S. & GRACE, J. R. 1999. Characteristic of Gas-
1040 Fluidized Beds in Different Flow Regimes. *Industrial & Engineering Chemistry*
1041 *Research*, 38, 803-811.
- 1042 BAKSHI, A., ALTANTZIS, C., BATES, R. B. & GHONIEM, A. F. 2015. Eulerian–
1043 Eulerian simulation of dense solid–gas cylindrical fluidized beds: Impact of
1044 wall boundary condition and drag model on fluidization. *Powder Technology*,
1045 277, 47-62.
- 1046 BEETSTRA, R., VAN DER HOEF, M. A. & KUIPERS, J. 2007. Drag force of
1047 intermediate Reynolds number flow past mono-and bidisperse arrays of spheres.
1048 *AIChE journal*, 53, 489-501.
- 1049 BELL, R. A. 2000. Numerical modelling of multi-particle flows in bubbling gas-solid
1050 fluidised beds, Swinburne University of Technology.
- 1051 BENYAHIA, S. 2008. Verification and validation study of some polydisperse kinetic
1052 theories. *Chemical Engineering Science*, 63, 5672-5680.
- 1053 BENYAHIA, S., SYAMLAL, M. & O'BRIEN, T. J. 2005. Evaluation of boundary
1054 conditions used to model dilute, turbulent gas/solids flows in a pipe. *Powder*
1055 *Technology*, 156, 62-72.
- 1056 CARDOSO, J., SILVA, V., EUS BIO, D., BRITO, P., BOLOY, R. M., TARELHO, L.
1057 & SILVEIRA, J. L. 2019. Comparative 2D and 3D analysis on the
1058 hydrodynamics behaviour during biomass gasification in a pilot-scale fluidized
1059 bed reactor. *Renewable Energy*, 131, 713-729.
- 1060 CARDOSO, J., SILVA, V., EUS BIO, D., BRITO, P. & TARELHO, L. 2018. Improved
1061 numerical approaches to predict hydrodynamics in a pilot-scale bubbling
1062 fluidized bed biomass reactor: A numerical study with experimental validation.
1063 *Energy Conversion & Management*, 156, 53-67.
- 1064 CHAO, Z., WANG, Y., JAKOBSEN, J. P., FERNANDINO, M. & JAKOBSEN, H. A.
1065 2012. Investigation of the particle–particle drag in a dense binary fluidized bed.
1066 *Powder technology*, 224, 311-322.
- 1067 COOPER, S. & CORONELLA, C. J. 2005a. CFD simulations of particle mixing in a
1068 binary fluidized bed. *Powder Technology*, 151, 27-36.
- 1069 COOPER, S. & CORONELLA, C. J. 2005b. CFD simulations of particle mixing in a
1070 binary fluidized bed. *Powder Technology*, 151, 27-36.

- 1071 CORONEO, M., MAZZEI, L. & LETTIERI, P. 2011. CFD prediction of segregating
1072 fluidized bidisperse mixtures of particles differing in size and density in gas–
1073 solid fluidized beds. *Chemical Engineering Science*, 66, 2317-2327.
- 1074 CORTES, C. & GIL, A. 2007. Modeling the gas and particle flow inside cyclone
1075 separators. *Progress in energy and combustion Science*, 33, 409-452.
- 1076 DING, J. & GIDASPOW, D. 2010. A bubbling fluidization model using kinetic theory
1077 of granular flow. *Aiche Journal*, 36, 523-538.
- 1078 DU, W., ZHANG, J., BAO, S., XU, J. & ZHANG, L. 2016. Numerical investigation of
1079 particle mixing and segregation in spouted beds with binary mixtures of
1080 particles. *Powder Technology*, 301, 1159-1171.
- 1081 ERGUN, S. 1952. Fluid flow through packed columns. *Chem. Eng. Prog.*, 48, 89-94.
- 1082 ESMAILI, E. & MAHINPEY, N. 2011a. Adjustment of drag coefficient correlations in
1083 three dimensional CFD simulation of gas-solid bubbling fluidized bed.
1084 *Advances in Engineering Software*, 42, 375-386.
- 1085 ESMAILI, E. & MAHINPEY, N. 2011b. Adjustment of drag coefficient correlations in
1086 three dimensional CFD simulation of gas–solid bubbling fluidized bed.
1087 *Advances in Engineering Software*, 42, 375-386.
- 1088 FAN, R. & FOX, R. O. 2008. Segregation in polydisperse fluidized beds: Validation of
1089 a multi-fluid model. *Chemical Engineering Science*, 63, 272-285.
- 1090 FENG, Y. & YU, A. 2007. Microdynamic modelling and analysis of the mixing and
1091 segregation of binary mixtures of particles in gas fluidization. *Chemical*
1092 *Engineering Science*, 62, 256-268.
- 1093 FORMISANI, B., GIRIMONTE, R. & VIVACQUA, V. 2011. Fluidization of Mixtures
1094 of Two Solids Differing in Density or Size. *Aiche Journal*, 57, 2325-2333.
- 1095 FOTOVAT, F., ANSART, R., HEMATI, M., SIMONIN, O. & CHAOUKI, J. 2015.
1096 Sand-assisted fluidization of large cylindrical and spherical biomass particles:
1097 Experiments and simulation. *Chemical Engineering Science*, 126, 543-559.
- 1098 GAN, J., HUI, Z., BERROUK, A. S., YANG, C. & SHAN, H. 2012. Impact of the drag
1099 law formulation on the predicted binary-particle segregation patterns in a gas–
1100 solid fluidized bed. *Powder Technology*, 218, 69-75.
- 1101 GAO, J., LAN, X., FAN, Y., JIAN, C., GANG, W., LU, C. & XU, C. 2009.

- 1102 Hydrodynamics of gas–solid fluidized bed of disparately sized binary particles.
1103 Chemical Engineering Science, 64, 4302-4316.
- 1104 GENG, S., JIA, Z., ZHAN, J., LIU, X., XU, G., GENG, S., JIA, Z., ZHAN, J., LIU, X.
1105 & XU, G. 2016. CFD modeling the hydrodynamics of binary particle mixture
1106 in pseudo-2D bubbling fluidized bed: Effect of model parameters. Powder
1107 Technology, 302, 384-395.
- 1108 GERA, D., GAUTAM, M., TSUJI, Y., KAWAGUCHI, T. & TANAKA, T. 1998.
1109 Computer simulation of bubbles in large-particle fluidized beds. Powder
1110 Technology, 98, 38-47.
- 1111 GERA, D., SYAMLAL, M. & O'BRIEN, T. J. 2004. Hydrodynamics of particle
1112 segregation in fluidized beds. International Journal of Multiphase Flow, 30,
1113 419-428.
- 1114 GIBILARO, L. G., FELICE, R. D., WALDRAM, S. P. & FOSCOLO, P. U. 1985.
1115 Generalized friction factor and drag coefficient correlations for fluid-particle
1116 interactions. Chemical Engineering Science, 40, 1817-1823.
- 1117 GIDASPOW, D., JUNG, J. & SINGH, R. K. 2004. Hydrodynamics of fluidization using
1118 kinetic theory: an emerging paradigm: 2002 Flour-Daniel lecture. Powder
1119 Technology, 148, 123-141.
- 1120 GIDASPOW, D., SYAMLAL, M. & SEO, Y. 1986. Hydrodynamics of fluidization of
1121 single and binary size particles: supercomputer modeling. Proceedings of
1122 fluidization V.
- 1123 GOLDSCHMIDT, M. J. V., KUIPERS, J. A. M. & SWAAIJ, W. P. M. V. 2001.
1124 Hydrodynamic Modeling of Dense Gas-Fluidized Beds Using the Kinetic
1125 Theory of Granular Flow: Effect of Coefficient of Restitution on Bed Dynamics.
1126 Chemical Engineering Science, 56, 571-578.
- 1127 HAIYING, Q. I., DAI, Q. & CHEN, C. 2014. The key scientific problems in the
1128 eulerian modeing of large-scale multi-phase flows-drag model. Mechanics in
1129 Engineering.
- 1130 HALVORSEN, B. M. & ARVOH, B. 2009. Minimum fluidization velocity, bubble
1131 behaviour and pressure drop in fluidized beds with a range of particle sizes. WIT
1132 Transactions on Engineering Sciences, 63, 227-238.
- 1133 HAMEED, S., SHARMA, A. & PAREEK, V. 2019. Modelling of particle segregation

- 1134 in fluidized beds. Powder Technology, 353, 202-218.
- 1135 HASSEN, W., THRIOUA, M., KOLSI, L., ANBUMALAR, V., AL-RASHED, A. &
 1136 BORJINI, M. N. 2018. CFD Modeling of Gas-Particles Flow in a Circulating
 1137 Fluidized G-Volution Gasification Reactor. International Journal of Mechanical
 1138 Sciences, S0020740318309056-.
- 1139 HOFFMANN, A. C., JANSSEN, L. P. B. M. & PRINS, J. 1993. Particle segregation in
 1140 fluidised binary mixtures. Chemical Engineering Science, 48, 1583-1592.
- 1141 HONG, K., SHI, Z., WEI, W. & LI, J. 2013. A structure-dependent multi-fluid model
 1142 (SFM) for heterogeneous gas–solid flow. Chemical Engineering Science, 99,
 1143 191-202.
- 1144 HUANG, A. N. & KUO, H. P. 2014. Developments in the tools for the investigation of
 1145 mixing in particulate systems – A review. Advanced Powder Technology, 25,
 1146 163-173.
- 1147 IDDIR, H. & ARASTOPOUR, H. 2005. Modeling of multitype particle flow using
 1148 the kinetic theory approach. Aiche Journal, 51, 1620–1632.
- 1149 JENKINS, J. T. & MANCINI, F. 1989. Kinetic theory for binary mixtures of smooth,
 1150 nearly elastic spheres. Physics of Fluids A Fluid Dynamics, 1, 2050-2057.
- 1151 JENKINS, J. T. & SAVAGE, S. B. 2006. A theory for the rapid flow of identical, smooth,
 1152 nearly elastic, spherical particles. Journal of Fluid Mechanics, 130, 187-202.
- 1153 JIAN, L. L. & LIM, E. W. C. 2017. Comparisons of Eulerian-Eulerian and CFD-DEM
 1154 simulations of mixing behaviors in bubbling fluidized beds. Powder Technology,
 1155 318.
- 1156 JOHNSON, P. C. & JACKSON, R. 1987. Frictional–collisional constitutive relations
 1157 for granular materials, with application to plane shearing. Journal of fluid
 1158 Mechanics, 176, 67-93.
- 1159 JUN, L. I., XUE, C. Z. & SONG, W. L. 2013. Hydrodynamics of a Freely Bubbling
 1160 Fluidized Bed Numerical Simulation Based on Particle-particle Drag Force
 1161 Model. Power System Engineering.
- 1162 KOCH, D. L. & HILL, R. J. 2001. I NERTIAL E FFECTS IN S USPENSION AND P
 1163 OROUS -M EDIA F LOWS. Annu.rev.fluid Mech, 33, 619-647.
- 1164 KONAN, N. A. & HUCKABY, E. D. 2017. Kinetic theory-based numerical modeling

- 1165 and analysis of bi-disperse segregated mixture fluidized bed. Powder
1166 Technology, 319, 71-91.
- 1167 LAN, X., XU, C., GAO, J. & AL-DAHMAN, M. 2012. Influence of solid-phase wall
1168 boundary condition on CFD simulation of spouted beds. Chemical Engineering
1169 Science, 69, 419-430.
- 1170 LI, J. & KWAIK, M. 2003a. Particle-fluid two-phase flow. China Particuology, 1, 42.
- 1171 LI, J. & KWAIK, M. 2003b. Particle-fluid two-phase flow. China Particuology, 1, 42-
1172 42.
- 1173 LI, T., GRACE, J. & BI, X. 2010. Study of wall boundary condition in numerical
1174 simulations of bubbling fluidized beds. Powder Technology, 203, 447-457.
- 1175 LIM, L. J. J. & LIM, E. W. C. 2019. Mixing and segregation behaviors of a binary
1176 mixture in a pulsating fluidized bed. Powder Technology, 345, 311-328.
- 1177 LIN, L. 2010. A Simulation Study of Gas-Solid Two Phase Flow in a Bubbling
1178 Fluidized Bed with Various Drag Force Models. Chemical Reaction
1179 Engineering & Technology, 26, 390-398.
- 1180 LU, H. & GIDASPOW, D. 2003. Hydrodynamics of binary fluidization in a riser: CFD
1181 simulation using two granular temperatures. Chem.eng.sci, 58, 3777-3792.
- 1182 LU, H., HE, Y. & GIDASPOW, D. 2003a. Hydrodynamic modeling of binary mixture
1183 in a gas bubbling fluidized bed using the kinetic theory of granular flow.
1184 Chemical Engineering Science, 58, 1197-1205.
- 1185 LU, H., HE, Y., GIDASPOW, D., YANG, L. & QIN, Y. 2003b. Size segregation of
1186 binary mixture of solids in bubbling fluidized beds. Powder Technology, 134,
1187 86-97.
- 1188 LU, H., YUNHUA, Z., DING, J., GIDASPOW, D. & WEI, L. 2007a. Investigation of
1189 mixing/segregation of mixture particles in gas–solid fluidized beds. Chemical
1190 Engineering Science, 62, 301-317.
- 1191 LU, H., ZHAO, Y., DING, J., GIDASPOW, D. & LI, W. 2007b. Investigation of
1192 mixing/segregation of mixture particles in gas–solid fluidized beds. Chemical
1193 Engineering Science, 62, 301-317.
- 1194 LUNGU, M., ZHOU, Y., WANG, J. & YANG, Y. 2015. A CFD study of a bi-disperse
1195 gas–solid fluidized bed: Effect of the EMMS sub grid drag correction. Powder

- 1196 Technology, 280, 154-172.
- 1197 LUO, Z. F., TANG, L. G., DAI, N. N. & ZHAO, Y. M. 2013. The effect of a secondary
1198 gas-distribution layer on the fluidization characteristics of a fluidized bed used
1199 for dry coal beneficiation. *International Journal of Mineral Processing*, 118, 28-
1200 33.
- 1201 MATHIESEN, V., SOLBERG, T., ARASTOPOUR, H. & HJERTAGER, B. H. 2010.
1202 Experimental and computational study of multiphase gas/particle flow in a CFB
1203 riser. *Aiche Journal*, 45, 2503-2518.
- 1204 MATHIESEN, V., SOLBERG, T. & HJERTAGER, B. H. 2000. Predictions of
1205 gas/particle flow with an Eulerian model including a realistic particle size
1206 distribution. *Powder Technology*, 112, 34-45.
- 1207 MAZZEI, L., CASILLO, A., LETTIERI, P. & SALATINO, P. 2010. CFD simulations
1208 of segregating fluidized bidisperse mixtures of particles differing in size.
1209 *Chemical Engineering Journal*, 156, 432-445.
- 1210 MCKEEN, TIM, PUGSLEY & TODD 2003. Simulation and experimental validation
1211 of a freely bubbling bed of FCC catalyst. *Powder Technology*, 129, 139-152.
- 1212 MCKEEN, T. & PUGSLEY, T. 2003. Simulation and experimental validation of a freely
1213 bubbling bed of FCC catalyst. *Powder Technology*, 129, 139-152.
- 1214 MOSTAFAZADEH, M., RAHIMZADEH, H. & HAMZEI, M. 2013. Numerical
1215 analysis of the mixing process in a gas–solid fluidized bed reactor. *Powder*
1216 *Technology*, 239, 422-433.
- 1217 MURRAY, J. D. 1965. On the Mathematics of Fluidization. Part I: Fundamental
1218 Equation and Wave Propagation. *Journal of Fluid Mechanics*, 21, 465-493.
- 1219 NIENOW, A., ROWE, P. & AGBIM, A. 1973a. Note on the liquid properties of gas
1220 fluidized-beds. *Transactions of The Institution of Chemical Engineers Inst*
1221 *Chemical Engineers 165-189 Railway Terrace, Davis Bldg, Rugby Cv21 3HQ.*
- 1222 NIENOW, A. W., ROWE, P. N. & AGBIM, A. J. 1973b. Note on the liquid properties
1223 of gas fluidized-beds. *Transactions of The Institution of Chemical Engineers.*
1224 *Inst Chemical Engineers 165-189 Railway Terrace, Davis Bldg, Rugby Cv21*
1225 *3HQ.*
- 1226 OWOYEMI, O., MAZZEI, L. & LETTIERI, P. 2007. CFD modeling of binary-
1227 fluidized suspensions and investigation of role of particle–particle drag on

- 1228 mixing and segregation. *AIChE journal*, 53, 1924-1940.
- 1229 OWOYEMI, O., MAZZEI, L. & LETTIERI, P. 2010. CFD modeling of binary-
 1230 fluidized suspensions and investigation of role of particle–particle drag on
 1231 mixing and segregation. *Aiche Journal*, 53, 1924-1940.
- 1232 PENG, L., LAN, X., XU, C., GANG, W., LU, C. & GAO, J. 2009. Drag models for
 1233 simulating gas–solid flow in the turbulent fluidization of FCC particles.
 1234 *Particuology*, 7, 269-277.
- 1235 PENG, Z., DOROODCHI, E., ALGHAMDI, Y. & MOGHTADERI, B. 2013. Mixing
 1236 and segregation of solid mixtures in bubbling fluidized beds under conditions
 1237 pertinent to the fuel reactor of a chemical looping system. *Powder Technology*,
 1238 235, 823-837.
- 1239 REDDY, R. K. & JOSHI, J. B. 2009. CFD modeling of solid–liquid fluidized beds of
 1240 mono and binary particle mixtures. *Chemical Engineering Science*, 64, 3641-
 1241 3658.
- 1242 RONG, F. & FOX, R. O. 2008. Segregation in polydisperse fluidized beds: Validation
 1243 of a multi-fluid model. *Chemical Engineering Science*, 63, 272-285.
- 1244 ROWE, P. 1972. The mechanisms by which particles segregate in gas fluidised beds-
 1245 binary system of near spherical particles. *Trans. Inst. Chem. Engng*, 50, 310-
 1246 323.
- 1247 ROWE, P. N. & NIENOW, A. W. 1976. Particle mixing and segregation in gas fluidised
 1248 beds. A review. *Powder Technology*, 15, 141-147.
- 1249 SANT'ANNA, M. C. S., CRUZ, W. R. D. S., SILVA, G. F. D., MEDRONHO, R. D. A.
 1250 & LUCENA, S. 2016. Analyzing the fluidization of a gas-sand-biomass mixture
 1251 using CFD techniques. *Powder Technology*, 316, S0032591016308907.
- 1252 SAVAGE, S. B. & JEFFREY, D. J. 2006. The stress tensor in a granular flow at high
 1253 shear rates. *Journal of Fluid Mechanics*, 110, 255-272.
- 1254 SHAH, M. T., MAYNE, J., UTIKAR, R. P., TADE, M. O. & PAREEK, V. K. 2010.
 1255 Gas–solid flow hydrodynamics of an industrial scale catalyst lift engager.
 1256 *Chemical Engineering Journal*, 159, 138-148.
- 1257 SHAH, M. T., UTIKAR, R. P., EVANS, G. M., TADE, M. O. & PAREEK, V. K. 2011a.
 1258 Effect of inlet boundary conditions on computational fluid dynamics (CFD)
 1259 simulations of gas–solid flows in risers. *Industrial & Engineering Chemistry*

- 1260 Research, 51, 1721-1728.
- 1261 SHAH, M. T., UTIKAR, R. P., TADE, M. O. & PAREEK, V. K. 2011b. Hydrodynamics
1262 of an FCC riser using energy minimization multiscale drag model. Chemical
1263 engineering journal, 168, 812-821.
- 1264 SHAH, M. T., UTIKAR, R. P., TADE, M. O., PAREEK, V. K. & EVANS, G. M. 2011c.
1265 Simulation of gas–solid flows in riser using energy minimization multiscale
1266 model: effect of cluster diameter correlation. Chemical engineering science, 66,
1267 3291-3300.
- 1268 SHARMA, A., WANG, S., PAREEK, V., HONG, Y. & ZHANG, D. 2014a. CFD
1269 modeling of mixing/segregation behavior of biomass and biochar particles in a
1270 bubbling fluidized bed. Chemical Engineering Science, 106, 264-274.
- 1271 SHARMA, A., WANG, S., PAREEK, V., YANG, H. & ZHANG, D. 2014b. CFD
1272 modeling of mixing/segregation behavior of biomass and biochar particles in a
1273 bubbling fluidized bed. Chemical Engineering Science, 106, 264-274.
- 1274 SINCLAIR, J. L. 1994. Fluidization: Idealized and bubbleless, with applications by M.
1275 Kwauk, ellis horwood, new york, 1992, 277 pp.,\$85.50. Aiche Journal, 40, 380-
1276 380.
- 1277 SITNAI, O. 1981. Solids mixing in a fluidized bed with horizontal tubes. Industrial &
1278 Engineering Chemistry Process Design & Development, 20, 533-538.
- 1279 SUN, L., LUO, K. & FAN, J. 2017. Numerical study on flow behavior of ultrafine
1280 powders in conical spouted bed with coarse particles. Chemical Engineering
1281 Research & Design, 125.
- 1282 SYAMLAL, M. 1987. The particle-particle drag term in a multiparticle model of
1283 fluidization. EG and G Washington Analytical Services Center, Inc.,
1284 Morgantown, WV (USA).
- 1285 SYAMLAL, M. & O'BRIEN, T. 1987. The derivation of a drag coefficient formula
1286 from velocity-voidage correlations. Technical Note, US Department of energy,
1287 Office of Fossil Energy, NETL, Morgantown, WV.
- 1288 TAGLIAFERRI, C., MAZZEI, L., LETTIERI, P., MARZOCHELLA, A., OLIVIERI,
1289 G. & SALATINO, P. 2013. CFD simulation of bubbling fluidized bidisperse
1290 mixtures: Effect of integration methods and restitution coefficient. Chemical
1291 Engineering Science, 102, 324-334.

- 1292 VEJAHATI, F., MAHINPEY, N., ELLIS, N. & NIKOO, M. B. 2009. CFD simulation
1293 of gas–solid bubbling fluidized bed: a new method for adjusting drag law. The
1294 Canadian Journal of Chemical Engineering, 87, 19-30.
- 1295 VENDERBOSCH, R. H. 1998. The role of clusters in gas-solids reactors an
1296 experimental study. Universiteit Twente: Enschede.
- 1297 WANG, F., YANG, B. X. & CHENG-JUN, J. I. 2009. Segregation of Multiple Solid
1298 Phases by Soft-sphere Simulation in Bubbling Fluidized Beds. Journal of
1299 Taiyuan University of Science & Technology.
- 1300 WANG, Q., JUNFU, L. U., YIN, W., YANG, H. & WEI, L. 2013. Numerical study of
1301 gas—solid flow in a coal beneficiation fluidized bed using kinetic theory of
1302 granular flow. Fuel Processing Technology, 111, 29-41.
- 1303 WANG, S., ZHANG, K., XU, S. & YANG, X. 2018. Assessment of a bubble-based bi-
1304 disperse drag model for the simulation of a bubbling fluidized bed with a binary
1305 mixture. Powder Technology, 338, 280-288.
- 1306 WANG, X., JIN, B., WANG, Y. & HU, C. 2015. Three-dimensional multi-phase
1307 simulation of the mixing and segregation of binary particle mixtures in a two-
1308 jet spout fluidized bed. Particuology, 22, 185-193.
- 1309 WANG, X., JIN, B., ZHONG, W. & XIAO, R. 2010. Modeling on the Hydrodynamics
1310 of a High-Flux Circulating Fluidized Bed with Geldart Group A Particles by
1311 Kinetic Theory of Granular Flow. Energy & Fuels, 24, 3159-3172.
- 1312 WANG, X. Z., WANG, T. Y., CHUN-TING, L. I., PENG, W. G. & LIU, W. T. 2012.
1313 Simulation of Particle Segregation Behavior in Bubbling Fluidized Bed. Energy
1314 Conservation Technology.
- 1315 WEI, D., ZHANG, J., BAO, S., JIAN, X. & ZHANG, L. 2016. Numerical investigation
1316 of particle mixing and segregation in spouted beds with binary mixtures of
1317 particles. Powder Technology, 301, 1159-1171.
- 1318 WEI, L., JIANG, G., TENG, H., HU, J. & ZHU, J. 2019. Multi-fluid Eulerian
1319 simulation of mixing of binary particles in a gas–solid fluidized bed with a
1320 cohesive particle–particle drag model. Particuology.
- 1321 WEN, C. Y. Mechanics of fluidization. Chem. Eng. Prog., Symp. Ser., 1966. 100-111.
- 1322 YANG, N., WANG, W., WEI, G. E. & JINGHAI, L. I. 2003. CFD simulation of
1323 concurrent-up gas-solid flow in circulating fluidized beds with structure-

- 1324 dependent drag coefficient. *Chemical Engineering Journal*, 96, 71-80.
- 1325 YINGCE, WANG, ZHENG, HONGZHONG & QINGSHAN 2014. A new drag model
1326 for TFM simulation of gas-solid bubbling fluidized beds with Geldart-B
1327 particles. *Particuology*, 15, 151-159.
- 1328 YUAN, P. T. & GIDASPOW, D. 1990. Computation of Flow Patterns in Circulating
1329 Fluidized Beds. *Aiche Journal*, 36, 885-896.
- 1330 ZAKI, W. & RICHARDSON, J. 1954. Sedimentation and fluidisation: Part I. *Trans.*
1331 *Inst. Chem. Eng.*, 32, 35-53.
- 1332 ZHANG, Y. & REESE, J. M. 2003. The drag force in two-fluid models of gas–solid
1333 flows. *Chemical Engineering Science*, 58, 1641-1644.
- 1334 ZHENG, X. Y., WEN-HAO, P. U., YUE, C., WEI-FENG, H. E. & HAN, D. 2015. A
1335 Modified Drag Model Used for CFD Simulation on the Fluidization
1336 Characteristics of 2D Bubbling Fluidized Bed. *Chinese Journal of Process*
1337 *Engineering*.
- 1338 ZHONG, H., GAO, J., CHUNMING, X. U. & LAN, X. 2012. CFD modeling the
1339 hydrodynamics of binary particle mixtures in bubbling fluidized beds: Effect of
1340 wall boundary condition. *Powder Technology*, 230, 232-240.
- 1341 ZHONG, H., LAN, X., GAO, J. & XU, C. 2014a. Effect of particle frictional sliding
1342 during collisions on modeling the hydrodynamics of binary particle mixtures in
1343 bubbling fluidized beds. *Powder Technology*, 254, 36-43.
- 1344 ZHONG, H., LAN, X., GAO, J. & XU, C. 2014b. Effect of particle frictional sliding
1345 during collisions on modeling the hydrodynamics of binary particle mixtures in
1346 bubbling fluidized beds. *Powder technology*, 254, 36-43.
- 1347 ZHONG, H., ZHENG, Y. & ZHANG, Z. 2016. 3D CFD simulation of instantaneous
1348 segregation process for binary particles. *China Powder Science & Technology*.
- 1349 ZHONGXI, CHAO, YUEFA, WANG, JANA, JAKOBSEN, MARIA, FERNANDINO,
1350 HUGO & JAKOBSEN 2012. Multi-fluid modeling of density segregation in a
1351 dense binary fluidized bed. *Particuology*, 10, 62-71.
- 1352 ZHU, H., ZHU, J., LI, G. & LI, F. 2008. Detailed measurements of flow structure inside
1353 a dense gas–solids fluidized bed. *Powder Technology*, 180, 339-349.
- 1354 ZIMMERMANN, S. & TAGHIPOUR, F. 2005. CFD Modeling of the Hydrodynamics

- 1355 and Reaction Kinetics of FCC Fluidized-Bed Reactors. *Industrial &*
 1356 *Engineering Chemistry Research*, 44, págs. 9818-9827.
- 1357 Haiying, Q. I., Q. Dai & C. Chen 2014. "The key scientific problems in the eulerian
 1358 modeling of large-scale multi-phase flows-drag model." *Mechanics in*
 1359 *Engineering*, 65, 2003-2012.
- 1360 Jun, L. I., C. Z. Xue & W. L. Song 2013. "Hydrodynamics of a Freely Bubbling
 1361 Fluidized Bed Numerical Simulation Based on Particle-particle Drag Force
 1362 Model." *Power System Engineering*, 21-23.
- 1363 Lin, L. 2010. "A Simulation Study of Gas-Solid Two Phase Flow in a Bubbling
 1364 Fluidized Bed with Various Drag Force Models." *Chemical Reaction*
 1365 *Engineering & Technology* 26(5): 390-398.
- 1366 Liu D. F., Zhang B. & Sun D. Z. 2016. "Numerical Simulation of Particle Flow
 1367 Characteristics in an Internal Swirling Fluidized Bed." *Energy Research &*
 1368 *Utilization*(5).
- 1369 Liu Y., Lu H. I., Liu W. T. & Zhao Y. H. 2003. "Model and simulation of gas-solid
 1370 flow with wide size distribution in circulating fluidized bed." *Journal of*
 1371 *Chemical Industry Engineering :China* 54(8): 1065-1071.
- 1372 Shao M. J., Lai Q. S. & Mooson Kwauk. 1991. "Particle mixing and separation moving
 1373 fluidized bed I. Behavior in the gravitational field." *Engineering Chemistry &*
 1374 *Metallurgy*.
- 1375 Tang Q. (2016). Numerical study on fluidization characteristics of multi-component
 1376 particles in circulating fluidized bed, Harbin Institute of Technology.
- 1377 Wang S. Y., Zhao Y. H., Jiang J., Liu G. D. & Chen H. L. 2007. "Numerical simulations
 1378 of effect of particle rotation on gas and solid flow behavior in fluidized beds."
 1379 *Journal of Engineering Thermophysics* 28(2): 262-264.
- 1380 Xiao H. T., Qi H. Y., You C. F. & Xu X. C. 2003. "Theoretical Model of Drag Between
 1381 Gas and Solid Phase." *Chinese J. Phys* 54(3): 311-315.
- 1382 Zhang K., Zhang J. Y. & Zhang B. J. 2004. "Simulation of fluid dynamics in a two-
 1383 component cold-model jet fluidized bed gasifier." *Journal of Fuel Chemistry*
 1384 32(6): 699-704.
- 1385 Zheng J. X. & Liu H. L. 2010. "Study on the influence of elastic restoration coefficient
 1386 on gas-solid flow field of ultrafine particles." *Journal of Northeast Electric*

- 1387 Power University 30(6): 10-14.
- 1388 Zheng X. Y., Pu W. H., Yue C., He W. F. & Han D. 2015. "Simulation of fluidization
1389 characteristics of 2D bubbling fluidized bed using improved drag model."
1390 Journal of Process Engineering 15(5): 737-743.
- 1391 Zhong H. B., Zheng Y. J. & Zhang Z. P. 2016. "Three-dimensional CFD simulation of
1392 transient grading process of two-component particles." China Powder
1393 Technology(4): 19-24.
- 1394 Zhu C. X., Zhang D. K., Zhao P. B., Wang H. T. & Gao H. P. 2009. "Effect of particle
1395 rotation on gas-solid two-phase flow characteristics in CFB." Clean Coal
1396 Technology 15(6): 61-63.
- 1397